AFOSR-TR- 79-0685

UNIVERSITY OF NEVADA - RENO - NEVADA - 89557

Mackay School of Mines
Seismological Laboratory

Telephone (702) 784-4975

LEVEL II

AD A070053

SEMIANNUAL
TECHNICAL REPORT NO. 3
3 APRIL 1979

ARPA Order No.	3291
Program Code	TF10-7F10
Name of Contractor	University of Nevada, Reno
Effective Date of Contract	01 February 1977
Contract Expiration Date	30 September 1978
Amount of Contract Dollars	$72,932
Contract Number	F49620-77-C-0070
Principal Investigator	Keith F. Priestley, 702-784-4975
Program Manager	Keith F. Priestley
Short Title of Work	SURFACE WAVES, SEISMIC REFRACTION AND UPPER MANTLE STRUCTURE OF THE BASIN AND RANGE

back copy
for 14 73

Sponsored by
Advanced Research Projects Agency (DOD)
ARPA Order No. 3291
Monitored by AFOSR Under Contract # F49260-77-C-0070

AIR FORCE OFFICE OF SCIENTIFIC RESEARCH (AFSC)
NOTICE OF TRANSMITTAL TO DDC
This technical report has been reviewed and is approved for public release IAW AFR 190-12 (7b).
Distribution is unlimited.
A. D. BLOSE
Technical Information Officer

Technical Report Summary

Body wave travel times, surface wave dispersion data, and gravity data are being studied to refine the structural details of the crust and upper mantle within the northern Basin and Range. Seismic refraction and Pn-delay data, and gravity data were used to examine variations in crustal thickness. The crust varies in thickness from 35-40 km in the vicinity of Mono Lake, to 28 km in the western part of the Battle Mountain heat flow high and 45 km in central Oregon. Higher mode Rayleigh wave group velocity data are in agreement with the thin crust in the northern Great Basin.

Details of the mantle lid structure have been examined using higher mode dispersion data. Phases identified as Sa or long-period Sn ($T \sim 13$ sec) are observed to have a phase velocity of 4.50 ± 0.03 k/s. The observed excitation and phase velocity of the Sa phase are in agreement with theoretical seismograms and computed phase velocity curves for the GREAT BASIN model. The agreement provides added support for the existence of a mantle lid of velocity 4.5 k/s and thickness about 30 km in the Great Basin. Fundamental and higher mode dispersion data for southern Nevada and Arizona indicate the structure of the southern Basin and Range is similar to that of the Great Basin.

Research Efforts

A. Refraction and gravity studies

Refraction data, array recordings of local and regional earthquakes and explosions, and gravity data have been used to derive a crustal model for the northwest Basin and Range Province. The Pg and Pn velocities were determined to be 6.1 k/s and 7.8 k/s respectively. No evidence was found for an intermediate crustal layer, however, $\overline{P}$ arrivals suggest an increase of velocity with depth in the crust. Array data indicate that the Pg and Pn velocities are relatively uniform over the northwest Basin and Range, hence variations in travel-times from NTS explosions and variations in the gravity field are interpreted primarily in terms of varying crustal thickness.

The single layer crustal model determined from the seismic and gravity data thins from approximately 35 km in the vicinity of Mono Lake, to 30 km along the Walker Lane east of Mono Lake, and to 30 km in the vicinity of Reno. The minimum crustal thickness of 28 km occurs near the southern boundary of the Carson Sink. North of the Carson Sink-Black Rock Desert area, the crust thickens to approximately 45 km in central Oregon. The gravity data is in agreement with the seismic model providing there is an increase in the average crustal density of 0.10-0.15 g/cc from the more acidic crust of central Nevada to the more basic crust of northwest Nevada and central Oregon. For details of this study see Appendix A.

B. Surface wave studies

Higher mode surface wave observations within the Great Basin of Nevada and western Utah have been analyzed. These consist of a Sa or long-period Sn phase observed for a number of earthquakes located off the coast of Oregon and Washington and crustal higher modes for moderate earthquakes located within the Great Basin.

The Sa phase has been identified as consisting primarily of the third higher Rayleigh mode and propagating with a significant energy content within the mantle lid. The energy is trapped within the lid by the natural positive velocity gradient resulting from the earth's sphericity. The 4.50 ± 0.03 k/s phase velocity of the Sa phase is in excellent agreement with the 4.50 k/s shear wave velocity of the lid determined from fundamental mode dispersion data. The 13 ± 2 sec predominant period of the Sa phase corresponds to wavelengths comparable to the thickness of the lid determined from the fundamental mode data. Thus this higher mode data provides strong support for the existence of the relatively thick mantle lid of the GREAT BASIN model (Priestley and Brune, 1978).

The crustal higher mode data indicates there are significant variations in the crustal thickness within the Great Basin. The fundamental mode data indicates an average crustal thickness of 35 km. However, across the northern Great Basin, the area of the Battle Mountain heat flow high, the crust is as thin as 23 km. For details of this study see Appendix B.

Surface wave data for the path Tucson, Arizon-Tonopah, Nevada has been analyzed. Fundamental mode Rayleigh and Love mode curves are shown in figure 1. These curves indicate the crustal and upper mantle structure of the southern Basin and Range is very similar to the structure of the Great Basin. The Sa phase discussed above propagates with little attenuation to Tucson indicating a mantle lid structure similar to that found in the Great Basin.

Field Efforts

A. Long-period seismic network: We are currently operating four WWSSN-type long-period seismic stations in the northern Basin and Range (fig. 2). Funding for operation of these stations is primarily from the National Science Foundation. These instruments are providing data for several studies. These include: (1) structure of the western Snake River Plane and Battle Mountain heat flow high from surface wave dispersion; (2) S-delay and S-to-P conversion studies; (3) long-period studies of regional Basin and Range earthquakes. Examples of data are shown in figure 3.

B. Battle Mountain reflection data: Seismic reflection data has been collected along a 30 km long line south of Battle Mountain, Nevada, using quary blast at the Copper Canyon mine as a seismic energy source (fig. 4). We have recently obtained a package of programs from R. B. Smith (University of Utah) for analysis of reflection data and have begun implimentation of these routines.

C. Snake River Plane refraction experiment: During September, 1978, a cooperative research effort for study of the seismic structure of the Snake River Plane was conducted. This included both United States and European universities and the U. S. Geological Survey. The University of Nevada with Scripps Institute of Oceanography (James Brune) deployed 25 instruments along a 250 km line crossing the northeastern Great Basin boundary with the Snake River Plane (fig. 2). Seismic energy generation was somewhat less than anticipated, however data from the shot point near Burley, Idaho was recorded to a distance of 200 km. Broad-band digital recordings in the

distance range 10-100 km should provide good estimates of attenuation in the volcanic crust. Some reversed data was recorded in the Jarbrige area from quary blast at Carlin, Nevada. Pn recordings from NTS test were made across the Great Basin-Snake River Plane boundary.

D. Attenuation Studies: Broad-band digital refraction data has been collected at a number of new sites along the Tonopah refraction profile described above. This data will provide information on upper mantle attenuation. We plan to record on additional tests in late spring. In addition to the NTS test, we have recorded several regional earthquakes for study of depth descriminants (fig. 2).

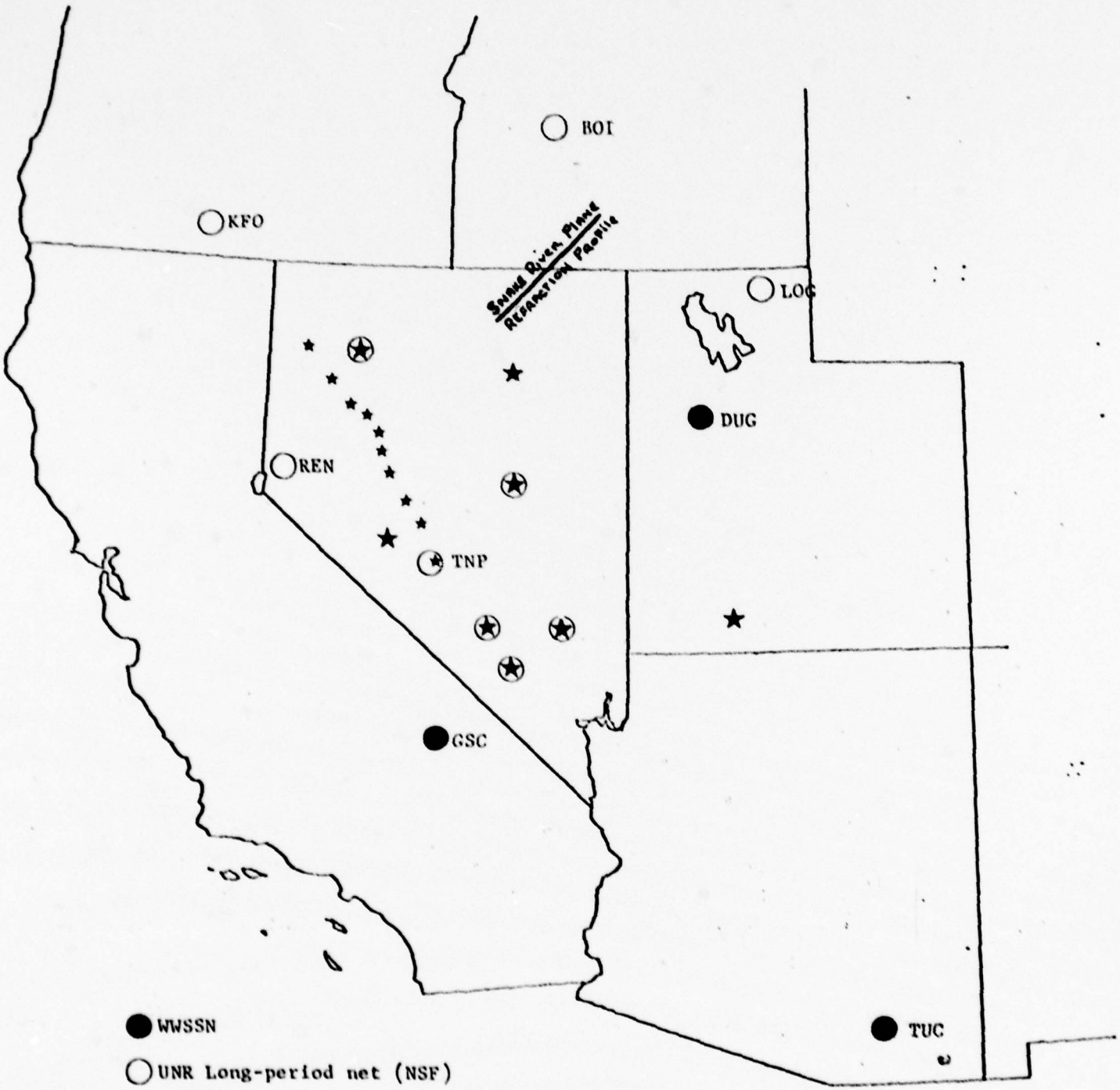
BOI
KFO
Snake River Plain
Refraction Profile
LOG
DUG
REN
TNP
GSC
TUC
WWSSN
UNR Long-period net (NSF)
UNR Broadband recording sites
LLL Broadband recording sites
Broadband refraction recording sites

Figure 1

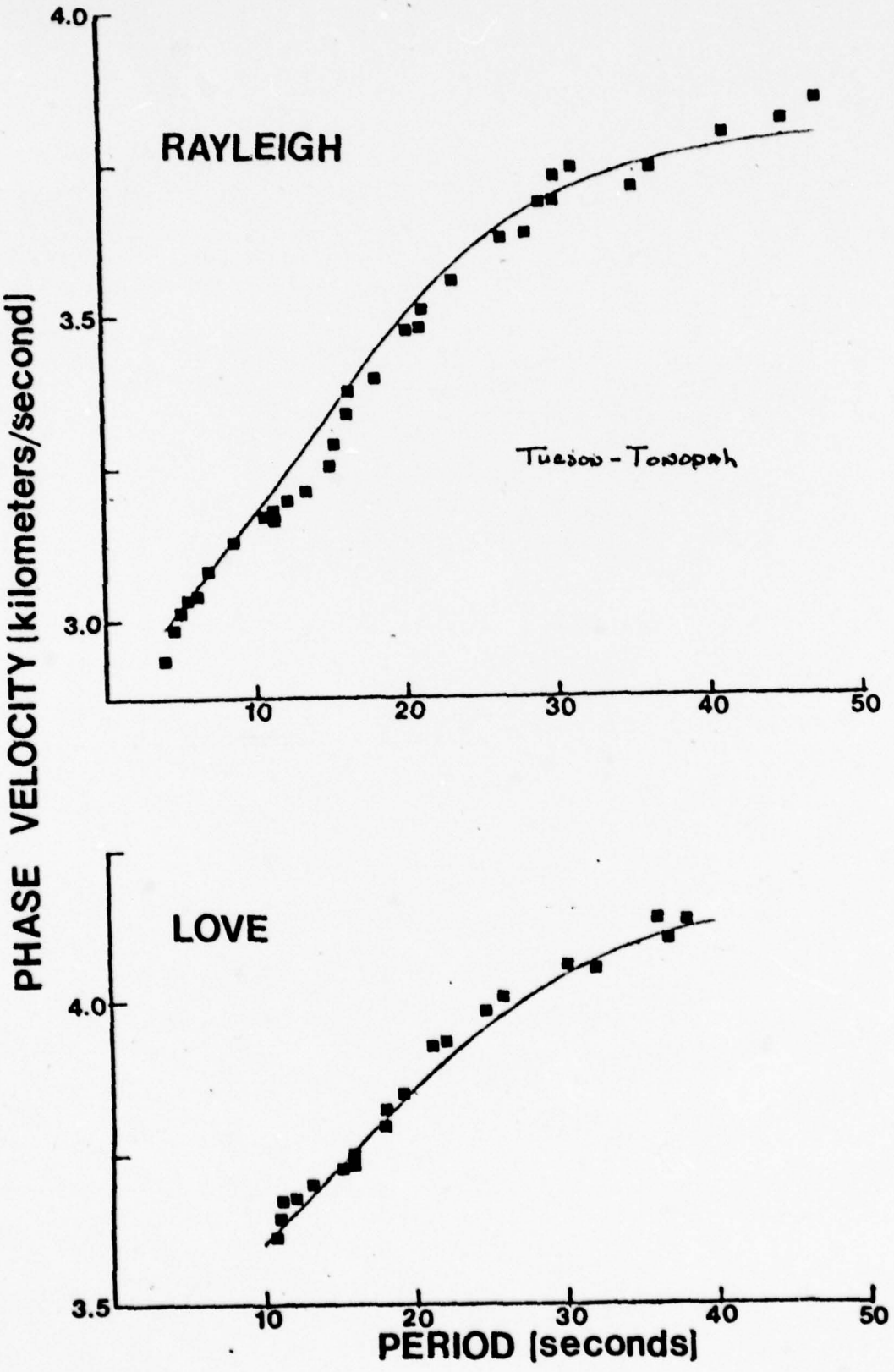
RAYLEIGH
Tucson - Tonopah
LOVE
PHASE VELOCITY [kilometers/second]
PERIOD [seconds]
4.0
3.5
3.0
4.0
3.5
10
20
30
40
50

fig 1.

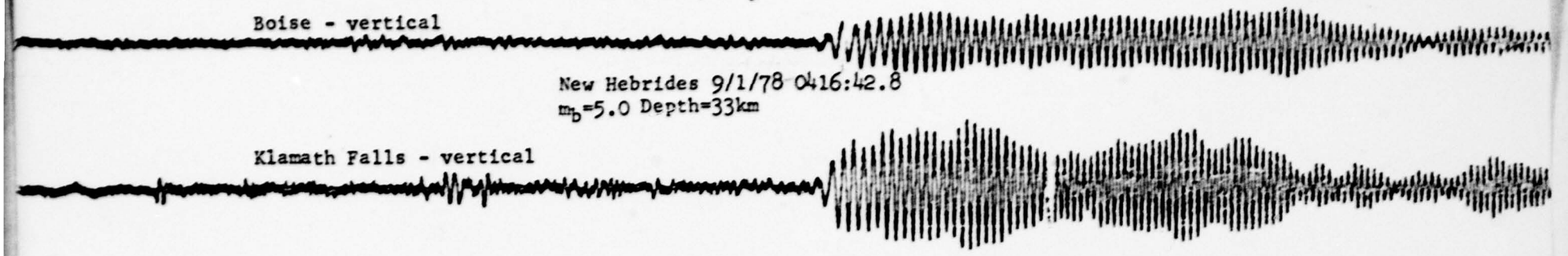

Figure 3. Long - period seismograms from northern Basin and Range.

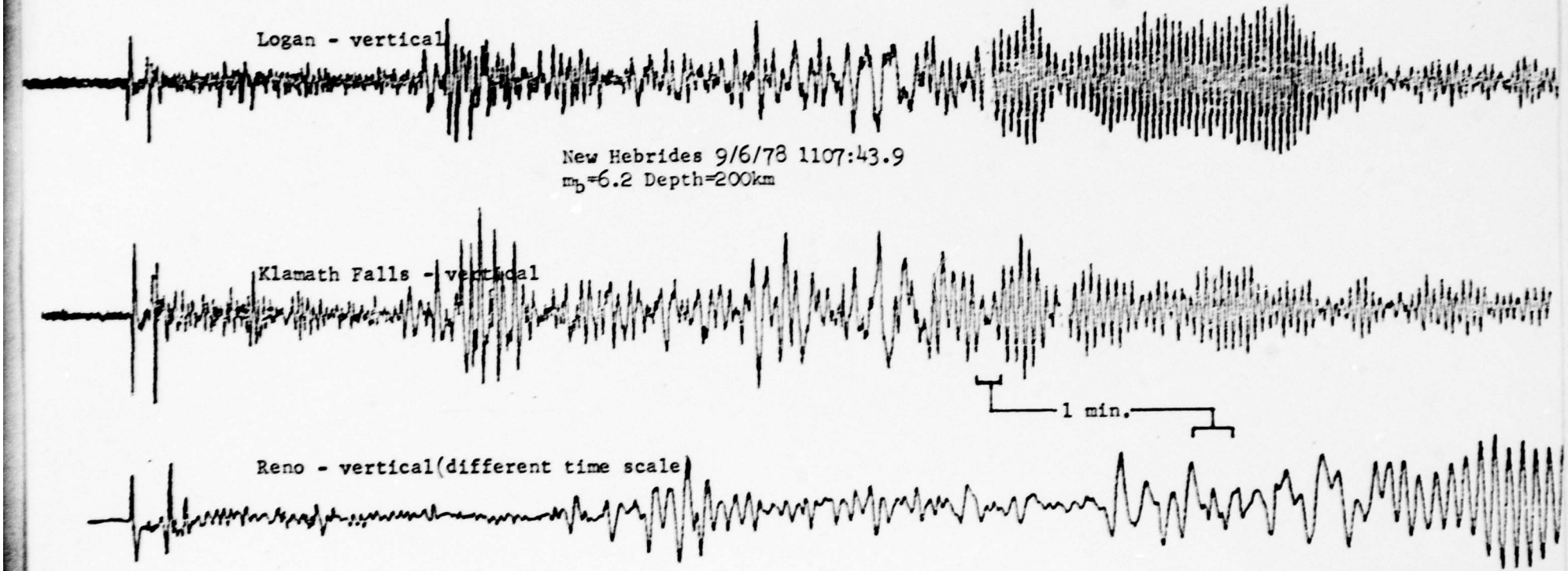

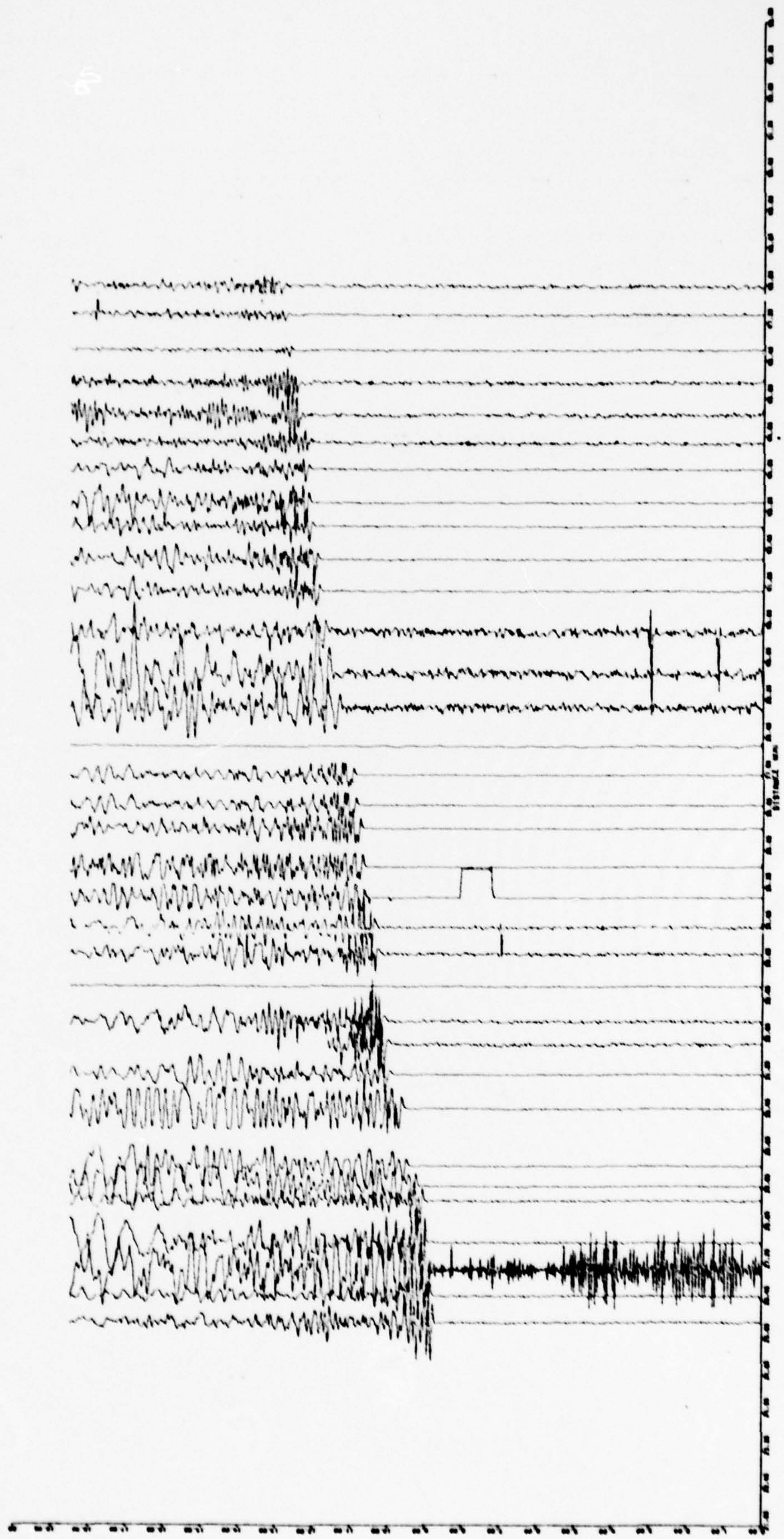

Appendix A

CRUSTAL STRUCTURE OF THE NORTHWESTERN BASIN AND RANGE PROVINCE

BY KEITH PRIESTLEY AND GLENN FEZIE

ABSTRACT

Refraction data, array recordings of local and regional earthquakes and explosions, and gravity data have been used to derive a crustal model for the northwest Basin and Range province. The crustal and upper mantle velocities were found to be 6.1 k/s and 7.8 k/s respectively. However, there is evidence for an increase in velocity with depth in both the crust and upper mantle. The average crustal thickness is 35 km. However, the crustal thickness varies from 40 km. in the vicinity of Mono Lake to 28 km. in the vicinity of the Carson Sink and 45 km. in central Oregon. The thin crust in the vicinity of the Carson Sink indicated by the refraction and gravity data in conjunction with results from heat flow measurements and geologic mapping indicate crustal stretching and intrusion as proposed by Lackenbruch and Sass (1978).

INTRODUCTION

Seismic waves generated by underground nuclear explosions at the Nevada Test Site (NTS) have been recorded along two unreversed profiles through western Nevada. These data and arrival times of well-recorded regional earthquakes and explosions at permanent seismic stations in western Nevada have been analyzed to determine the crustal structure and upper mantle P-wave velocity in the northwestern Basin and Range province. This region includes the western Nevada seismic zone, the western portion of the Battle Mountain heat flow high, and the Great Basin boundary with the volcanic province of eastern Oregon.

Previous seismic refraction work in this area consists of two reversed and two unreversed profiles using chemical explosions as a seismic source. Eaton (1963) reported results for a reversed profile from shot points at Fallon and Eureka, and for unreversed profiles from Fallon, west across the Sierra Nevada Mountains near Reno, and from Fallon south into Owens Valley. Johnson (1965) reported results for a reversed profile from Mono Lake to Lake Mead. The locations of these profiles are shown in figure 1. The time-term study of Batra (1970) included results from four stations within our area of study.

DATA

Refraction Data: Seismograph placement along the two profiles is shown in figure 1. The first profile extends 600 km. from near

Tonopah, Nevada (150 km. north of NTS) across the Lahontan Depression and into south-central Oregon. The second profile extends 200 km. from southeast of Hawthorne, Nevada (190 km. northwest of NTS) to Reno. The Pg-Pn cross-over distance within this area of the Basin and Range is typically 150 km. Thus, first arrivals along both profiles with the possible exception of recordings near Tonopah, are Pn. All recording sites are on or very near bedrock outcrops so as to minimize near surface and sedimentary effects.

Three recording systems have been used in the refraction experiment. Signals from 1 Hz vertical component seismometer were recorded on a portable, FM-tape recording telemetry system and on smoke paper recorders. Signals from three-component 10 second seismometers were recorded on broadband digital recorders developed at the University of Nevada (Peppin and Bufe, 1979). WWVB time code broadcast by the National Bureau of Standards is also recorded on the FM and digital tape for accurate time correlation between stations. The timing accuracy of the data from magnetic tape is $\pm$ 0.01 seconds; that from the smoke paper records is $\pm$ 0.05 seconds.

Network Data: The University of Nevada has operated a number of short period seismic stations in western Nevada to monitor microearthquake activity in the western Great Basin (figure 1). Signals from these stations are transmitted to Reno and recorded on analog magnetic tape along with WWVB. In addition to microearthquakes, a

large number of regional earthquakes and explosions have been recorded. Arrival times from well-recorded events (table 1) have been analyzed to determine the Pg and Pn velocities, and crustal delays. Similar studies using events outside seismograph arrays have been conducted by Kind (1972) in California and McCollom and Crosson (1975) in Washington.

Data Corrections: The datum for this study is a plane 1.5 km. above sea level--the average elevation of the shot points and recording sites. All first arrival times have been corrected for elevation to yield arrival times expected for recordings at the datum using a near-surface velocity of 4.5 k/s. Shot point coordinates and origin times were adjusted so as to make arrival times from the different explosions consistent at permanent stations along the profile.

VELOCITY DETERMINATION

Refraction Study: First arrival times on seismic records corrected for variations in recording site elevation and shot point coordinates are plotted in figure 2. The first arrival data for the Hawthorne profile is fit by the line

$$T = 6.78 + \Delta/7.90$$

and is interpreted as being Pn, the critically refracted headwave travelling in the uppermost mantle below the M-discontinuity. First arrivals for the Tonopah profile in the distance range 150 km. to 390 km. are fit by the line

$$T = 6.54 + \Delta/7.89$$

and are also interpreted as Pn. At distances greater than approximately 400 km. on the Tonopah profile the first arrival is fit by the line

$$T = 3.28 + \Delta/7.46$$

There is a suggestion of several phases following the first arrival in the distance range 375 to 475 km. (Fig. 3). The most prominent is a phase with apparent velocity 6.25 k/s. The large amplitude and extended coda of this phase suggest that it is $\overline{P}$ (Ryall and Stuart, 1963; Hill, 1972). This crustal phase involves multiple critical reflection between the surface and the M-discontinuity and provides an estimate of the average crustal velocity. The Pg velocity was not determined from the refraction data.At near distances Pn is clipped and Pg cannot be seen; at greater distances it is

obscured by the $\overline{P}$ wave train.

The slope of the above lines gives an estimate of the phase velocity of northward propagating Pn. This value is dependent on both the upper mantle velocity and the crustal delay terms. These effects are not separable with unreversed data. The simplest interpretation is that of a flat lying, plane layered structure with the phase velocities given above corresponding to the true upper mantle velocity. However, previous refraction results suggest the upper mantle velocity within the western Great Basin is somewhat lower than 7.9 k/s as indicated above. The Pn velocity from both reversed refraction profiles in this region (Eaton, 1963; Johnson, 1965) is near 7.8 k/s. Pn velocities determined by averaging refraction data for profiles of widely varying azimuth are 7.84 k/s (Ryall and Jones, 1964) and 7.8 k/s (Priestley and Brune, 1978). The phase velocity of first arrivals from the August, 1978 Mt. Shasta earthquakes recorded at several stations southward along the Tonopah profile is 7.7 ± 0.05 k/s These results suggest that the uppermost mantle P-wave velocity is near 7.8 k/s and the higher apparent velocity from our NTS refraction data for distances less than 400 km is due to a 1^{o} dip to the M-discontinuity towards the south.

The Pn phase velocity observed at distances greater than approximately 400 km. along the Tonopah profile is 7.4 k/s--extremely low for the upper mantle. Since there are no reversed Pn recordings

in this area, it is not possible to distinguish between velocity variations due to changes in upper mantle properties and apparent velocity variations due to changes in crustal structure. Low Pn velocities have been observed across the northern Great Basin(Batra, 1970; Boore and Stauber-personal communications, 1978; Braile-personal communication, 1978).

The phase velocity of Pa (Bath and Arroyo, 1963) or long period Pn has been measured southward along the path Reno to Tonopah. Both short-period and long-period recordings were available so the phase velocity as a function of period could be estimated. The results are given in table 2. Priestley and Brune (1978) and Priestley et al (1979) have shown evidence from fundamental and higher mode surface wave dispersion data for a relatively thick mantle lid in the central Great Basin. Burdick and Helmberger (1978) have found similar evidence from P-wave data for the interior western United States. Assuming the Pa phase propagates in the mantle lid in a similar manner to the Sa phase (Priestley, et al, 1979), the increase in velocity with period suggest an increase in velocity with depth in the mantle lid. Thus the low average Pn velocity observed for high frequency refraction data probably applies to the upper portions of the mantle lid and the Pa data suggest a positive velocity gradient with depth within the lid.

Network study: To estimate the true Pn velocity within the western Great Basin we have analyzed arrival time data from regional earthquakes and explosions covering a wide range of azimuths, and recorded at permanent western Nevada seismic stations. Arrival times for events of table 1 were first plotted against epicentral distance and a least-squares curve fit to the data to check that events lay within the Pn range. The slope of this curve provides an estimate of the phase velocity of the first arrivals across the seismic network as a function of azimuth.

Two numerical procedures were used to analyze the network data. First we have used a modified time-term approach (Willmore and Bancroft, 1960; McCollom and Crosson, 1975) to analyze a subset of the network data. As normally applied, this method allows one to estimate the refraction velocity and station delays terms by solving the time-term equation

$$T_{ij} = A_i + B_j + \Delta_{ij}/v$$

where T_{ij} and Δ_{ij} are the observed travel-time and epicentral distance of the i^{th} event recorded at the j^{th} station, A_i and B_j are the event and receiver site delays respectively, and v is the refraction velocity. For a complete solution, at least one event and receiver occupy the same site, a requirement not satisfied by our data. Therefore, we have determined only the refractor velocity. The time-term method assumes a horizontal, plane layered structure with velocities constant in the layers. Bath (1978) has shown the

magnitude of errors to be expected when these assumptions are violated. For the determination of refractor velocity, the most critical is the errors introduced by a dipping interface. The error is proportioned to cos γ where γ is the dip of the interface. For the region under consideration, the dip of the M-discontinuity does not exceed 3^{o} which corresponds to a maximum error of $\pm$ 0.01 km/sec in the determined velocity.

In addition, we have employed the method described by Kind (1972) for evaluating the refraction velocity and an azimuthally independent set of station residuals. The travel-time residuals R_{ij} of the i^{th} event as recorded at the j^{th} station are assumed to consist of two parts: $R_{ij} = a_{ij} + b_j$ where b_j is the station residual which is the same for all events recorded at the j^{th} station and a_{ij} is a value which varies with station and event such that $\sum_{i=1}^{m} a_{ij} = 0$. Then the azimuthally independent station residual is given by

$$b_j = \frac{1}{m} \sum_{i=1}^{m} R_{ij}$$

The travel-time residuals have been determined by fitting a least-squares line to the first arrival data from a set of events well-distributed in azimuth. The residuals R_{ij} are then the difference between the observed and predicted arrival times. The values of the station residuals b_j were then computed and these values were subtracted from the observed data. The process was then repeated

until the adjustments in the computed refraction velocity and station residuals became small.

These methods were applied to subsets of first arrival data for events of table 1; the results are summarized in table 3. A limited number of NTS events were used so as to not bias the data from this azimuth. The upper mantle velocity is 7.81 $\pm$ 0.04 k/s, in agreement with previous results (Eaton, 1963; Ryall and Jones, 1964; Johnson, 1965). The crustal velocity is 6.05 $\pm$ 0.05 k/s in agreement with earlier crustal velocities determined in the Great Basin.

CRUSTAL STRUCTURE

The travel-time data in figure 2 are unreversed and it is not possible to determine the upper mantle p-wave velocity unambiguously from the observed phase velocity. Variations in the travel-time along the profile may result from variations in the crustal delays due to changes in the crustal thickness or crustal velocity, or from variations in the upper mantle velocity. We find the crust and upper mantle velocities to be 6.1 k/s and 7.8 k/s respectively, in agreement with previous results (Eaton, 1963; Ryall and Jones, 1964; Johnson, 1965) and find no evidence for large or systematic deviations from these values. Assuming the velocities are constant, the Pn delay times provide a direct measure of the variation in crustal thickness.

The Pn phase velocities determined along the Hawthorne profile, and along the Tonopah profile at distances less than 400 km., are 7.90 k/s and 7.89 k/s respectively. Assuming and upper mantle velocity of 7.8 k/s, these phase velocities indicate approximately 4 km. of crustal thinning along these parts of the paths. Figure 4a is a reduced travel-time plot of the Tonopah profile data. These delay terms contain information on the crustal thickness at both the source and receiver site. The variation in the delay terms reflect variations in crustal thickness along the profile.

Figure 4b is an equivalent single layer crustal model computed from the delay terms of figure 4a assuming: (1) an average crustal p-wave velocity of 6.25 k/s based on the $\overline{P}$ velocity; (2)

an upper mantle p-wave velocity of 7.80 k/s; and (3) a crustal thickness of 24 km. at Fallon (Eaton, 1963). A single layer crustal model was determined since P* is nowhere a first arrival nor are there strong second arrivals corresponding to P* within the western Great Basin. This approximation will introduce a small error into the determined crustal thickness and the horizontal distance at which the Pn ray emerges from the mantle. However, since the intermediate layer does not appear to be well-developed in the western Great Basin, this error should not exceed a few percent.

Under these assumptions, the Pn delays indicate the crust decreases in thickness from 34 km. near Tonopah to 28 km. at the southern boundary of the Carson Sink. Across the Carson Sink there is 4 km. thinning of the crust corresponding to the 0.4 seconds advance in the travel time shown in figure 4a. This thinning occurs over a distance of 30 km. between stations on the north and south side of the sink. Since bedrock recordings cannot be made across the Carson Sink, it is not possible to determine whether the offset is the result of abrupt crustal thinning resulting from a fault offset in the M-discontinuity or a gradual thinning over the 30 km. distance. The thinning occurs either south of or at the southern boundary of the Carson Sink, since the Pn arrivals recorded on the north side of the sink emerge from the mantle 30 to 35 km. south of the recording site.

North of the Carson Sink, the first arrival is slow in velocity, and in the distance range 420 to 500 km., is weak in amplitude. The Pg velocity in northwest Nevada is 6.1 k/s. Assuming the Pn velocity is 7.8 k/s as in the west central Great Basin, and that the first arrival is Pn, the slower phase velocity is a manifestation of crustal thickening. These assumptions were applied in constructing the model for this area in figure 4b. However, the nature of the seismogram in the distance range 420 to 500 km. indicates the structure may be somewhat more complex. In this distance range, figure 2 shows evidence for a stronger, higher velocity phase following the first arrival. There are several possible explanations for this complication, none of which can be adequately resolved by our seismic data. These possibilities include: (1) The first arrival is diffracted energy from a zone of rapid crustal thickening with the second higher velocity phase being the refracted upper mantle arrival; (2) Arrivals in this distance range may be the manifestation of a shadow zone resulting from a velocity inversion in the lower crust or upper mantle; (3) The higher velocity arrivals represent laterally refracted energy. These possibilities cannot be adequately resolved with the available seismic refraction data, however, other geophysical data (primarily gravity) can aid in resolving the ambiguity.

The crustal model shown in figure 4b is in good agreement with surface wave dispersion results for the Great Basin. The average

crustal thickness for the central Great Basin determined from fundamental mode surface wave dispersion is 35 km. (Priestley and Brune, 1978). The group velocity of the second higher Rayleigh mode has been measured along the same path as the Tonopah refraction profile (Priestley et al, 1979). The average crustal thickness between the epicenter of the Adel, Oregon earthquake (Δ = 640 km. on the refraction profile) and Tonopah (Δ = 150 km.) is 31 km., in reasonable agreement with the average crustal thickness from the refraction data.

Gravity data provides an independent check on the variations in crustal properties. Figures 4c-f compare the free air and Bouguer gravity observed along the profile with the surface elevation and the expected Bouguer gravity computed from the crustal model in figure 4b. The gravity and elevation data are from the National Solar and Terrestrial Data Center with supplemental gravity data recorded by the authors. The gravity and elevation data have been smoothed by computing a 50 km. moving average to remove near surface effects in the gravity data and to provide the regional trend of the elevation. The theoretical gravity has been determined using a simple slab over a half-space calculation from the seismic structure using the Nafe-Drake relationship between seismic velocity and density (Grant and West, 1965).

In general, the free air anomaly is a direct measure of the degree of isostatic compensation. The free air gravity along the

refraction profile deviates little from zero, indicating approximate isostatic equilibrium. Low values occur in the distance range 300 to 400 km. and correspond to the mass deficiency associated with the deep sediment accumulation of the Carson Sink. The Bouguer anomaly shows an inverse relationship to the regional elevation. Since the effects of mass above sea level have been removed, the Bouguer anomaly is associated with deeper mass distributions and the effects of variations in crustal thickness and composition.

The effects of sediment accumulation in the Carson Sink must be removed from the observed gravity to see the effects of deeper crustal structure. From the free air anomaly, there is approximately a 30 milligal deficiency over the Carson Sink. In computing the Bouguer correction a density of 2.67 g/cc is assumed for the near surface rock. The average density of the shallow sediments is near 2.0 g/cc. Therefore, in making the Bouguer correction approximately 25 milligals too much was subtracted off. In addition, the low density sediments below sea level contribute another 30 to 35 milligals. Thus the Bouguer values should be 55 to 60 milligals more positive than shown in figure 4d. The estimated Bouguer curve after accounting for the sedimentary deposits is shown by the dashed line in figure 4d.

The Bouguer gravity computed from the seismic model (figure 4e) is in reasonable agreement with the modified gravity of figure

4d to a distance of 450 to 500 km. North of this point the fit becomes progressively worse. The surface geology (Stewart and Carlson, 1976) indicates the Carson Sink vicinity is roughly the boundary between the more acidic crust of central Nevada and the more basic crust of northwest Nevada and central Oregon. By reducing the crust-mantle density contrast by 0.10-0.15 g/cc in the area of basaltic composition, the computed Bouguer gravity is brought into better agreement with the observed Bouguer gravity. In northwest Nevada and south-central Oregon the crust is thicker and the lower average elevation results from compensation of a denser crustal section.

These results can be compared with other published refraction results across the central and northern Great Basin (Hill and Pakiser, 1966; Stauber and Boore, 1978). The relationship of our refraction profiles to these earlier refraction profiles is shown in figure 1. The observations of Hill and Pakiser (1966) include both reversed recordings over short segments, and unreversed recordings of NTS nuclear explosions over a profile extending from Eureka, Nevada to Boise, Idaho. From the reversed refraction data they determined the upper and lower crustal velocities to be 6.0 k/s and 6.7 k/s, respectively, and the upper mantle velocity to be 7.9 k/s. Along this profile, the crust thins from approximately 35 km. thick south of Eureka to less than 30 km. thick in the vicinity of Elko. The crust thickens northward from Elko to approxi-

mately 50 km. in the vicinity of Boise. Stauber and Boore (1978) interpreted unreversed refraction data from NTS nuclear explosions as indicating a thinning of the crust from 30 km. in the vicinity of Austin to 21 to 23 km. in the Battle Mountain-Winnemucca area. Seismic reflection data and gravity data further substantiate the thin crust in the Battle Mountain-Winnemucca area.

The results of Hill and Pakiser (1966) and Stauber and Boore (1978) in conjunction with the results of this study present a consistent model of crustal thinning along the northern boundary of the Great Basin.

We have used Pn arrival times from NTS events recorded at permanent western Nevada seismic stations to examine lateral variations in the crustal structure within the western Great Basin. Only NTS events were used since their origin times are accurately known and the impulse first arrivals can be accurately timed. Reduced travel-times for the NTS events of table 1 were computed for each recording site. Relative residuals were then determined by subtracting the delay-times of the station near Mono Lake from the residuals at the other sites. This removes the effects of variations in structure between different shot points. The delay-terms from all events at each site were then averaged and these values are plotted in figure 5a. Figure 5b is a contour map of equivalent crustal thickness computed from the delay-terms assuming a single layer crust of average p-wave velocity 6.25 k/s overlying a mantle

of p-wave velocity 7.8 k/s. All values have been plotted at the point where the Pn ray emerges from the mantle.

Figures 5c and 5d are the smoothed free air and Bouguer gravity respectively. The free air gravity averages near zero indicating the area is in approximate isostatic equilibrium. The Bouguer gravity is negative; however, there is an absolute low of -230 milligals in the vicinity of Mono Lake and a relative high of -150 milligals in the vicinity of Lovelock. The Bouguer gravity low shows a mass deficiency in the area of positive Pn residual and thicker crust while the relative high shows a relative mass excess in the vicinity of early residual and thin crust.

These results are in reasonable agreement with the unreversed refraction observations of Eaton (1963) within the same region. For the unreversed profiles south and west of Fallon, the average crustal thickness was 34.5 km. and 34 km. respectively. From reversed refraction data, the crustal thickness at the Fallon shot point was determined as 24 km. given a crustal thickness of 45 km. in the northern Owens Valley and 43 km. beneath the crest of the Sierra Nevada mountains. However, PmP reflection data along the two profiles suggested the crustal thickening along the Fallon-Owens Valley profile took place within 50 km. of the Fallon shot point and along the Fallon-Sierra Nevada profile took place abruptly 40 km. west of Fallon. Our Pn delay data suggest the crustal

thickening takes place both south and west of the points suggested by Eaton.

SUMMARY AND DISCUSSION

We have examined the structure of the crust and upper mantle of the northwest Basin and Range province using refraction data from the Nevada Test Site, network recordings of earthquakes and explosions, and gravity data. The Pg and Pn velocities were determined to be 6.1 k/s and 7.8 k/s respectively. No evidence was found for an intermediate crustal layer, however, $\overline{P}$ arrivals suggest an increase of velocity with depth in the crust. Array data indicate that the Pg and Pn velocities are relatively uniform over the northwest Basin and Range, hence variations in travel-times from NTS explosions and variations in the gravity field are interpreted primarily in terms of varying crustal thickness.

The single layer crustal model determined from the seismic and gravity data thins from approximately 40 km. in the vicinity of Mono Lake, to 30-35 km. along the Walker Lane east of Mono Lake, and to 30 km. in the vicinity of Reno. The minimum crustal thickness of 28 km. occurs near the southern boundary of the Carson Sink. North of the Carson Sink-Black Rock Desert area, the crust thickens to approximately 45 km. in central Oregon. The gravity data is in agreement with the seismic model providing there is an increase in the average crustal density of 0.10-0.15 g/cc from the more acidic crust of central Nevada to the more basic crust of northwest Nevada and central Oregon.

The thinner crust found in the northern Great Basin coincides with the western portion of the Battle Mountain heat flow high (Sass et al, 1976). Suppe et al, (1975), Smith (1977) and Lackenbruch and Sass (1978) have suggested that the northern Great Basin is a zone of crustal rifting. Priestley and Brune (1978) have shown the mantle shear wave structure of this area to be similar to that found in other areas of crustal rifting. McKenzie (1978) has proposed a simple mathematical model representing such a zone. In this stretching model, the lithosphere is extended and thinned, resulting in an upwelling of warm asthenospheric material with a resulting rise in the geothermal gradient. Since the lithosphere is isostatically compensated throughout the process, there is an initial subsidence associated with rifting. If the volcanic activity 16-17 m.y.B.P. marks the initiation of rifting, the subsidence and heat flux now observed indicate a stretching of the lithosphere by a factor of 2. The geology (Stewart and Carlson, 1976; Schilling-personal communications, 1979) indicates the rifting process is somewhat more complicated than the simple model of McKenzie (1978). The subsurface basaltic intrustions and buried basalt flows found in the vicinity of the Carson Sink suggest that, at least in this area, part of the extension is accommodated by intermittent basaltic intrusions into the crystalline crust (Lackenbruch and Sass, 1978).

ACKNOWLEDGMENTS

The authors are indebted to Eric Broten, David Chavez, Walter Nicks, John Stabile, Austin Wilson, Amy Mohler, and Doug VanWormer, for assistance in recording the refraction data, and to John Erwin for loan of the Worden gravimeter. We have benefited from discussions with James Brune, William Peppin, and Alan Ryall. This research has been supported by the Advanced Research Projects Agency and was monitored by the Air Force Office of Scientific Research under contract F49-620-77-C-0070, and by the U. S. Geological Survey under grant 14-08-0001-G-432.

REFERENCES

Bath, M. and A. L. Arroyo (1963). Pa and Sa waves and the upper mantle, Geofir. Pura e. Appl., 56, 67.

Bath, M. (1978). An analysis of the time-turn method in refraction seismology, Tectonophysics, 51, 155.

Batra, R. (1970). Travel-times and structure in the Nevada region from earthquakes, nuclear explosions, and mine blasts, M.S. Thesis, University of Nevada, Reno.

Burdick, L. and D. Helmberger (1978). The upper mantle P velocity structure of the western United States, J. Geophys. Rev., 83, 1699.

Eaton, J. P. (1963). Crustal structure from San Francisco, California, to Eureka, Nevada, from seismic refraction measurements, J. Geophys. Rev., 68, 5789.

Grant, F., and G. West (1965). Interpretation theory in applied geophysics, McGraw-Hill, New York.

Hill, D. and L. Pakiser (1966). Crustal structure between Nevada Test Site and Boise, Idaho, in The Earth Beneath the Continents: Am. Geophys. Union, Geophys. Mon. 10, 391.

Hill, D. (1972). Crustal and upper mantle structure of the Columbia Plateau from lang range seismic-refraction measurements, Geol. Soc. Am., 83, 1939.

Johnson, L. (1965). Crustal structure between Lake Mead, Nevada and Mono Lake, California, J. Geophys. Res., 70, 2863.

Kind, R. (1972). Residuals and velocities of Pn waves recorded by the San Andreas seismograph network, Bull. Seis. Soc. Am., 65, 85.

Koizumi, C. J., A. Ryall, and K. F. Priestley (1973). Evidence for a high-velocity lithospheric plate under northern Nevada, Bull. Seis. Soc. Am., 63, 2135.

Lackenbruch, A., and J. Sass (1978). Heat flow in the United States and the thermal regions of the crust, in Heacock, J. G., ed., The Nature and Physical Properties of the Crust: Geophys. Mon. Ser., 20, 626.

McCollom, R. L., and R. S. Crosson (1975). An array study of upper mantle velocity in Washington State, Bull. Seis. Soc. Am., 65, 467.

McKenzie, D. (1978). Some remarks on the development of sedimentary basins, Earth and Planetary Science Letters, 40, 25.

Peppin, W., and C. G. Bufe (1979). Induced (?) versus natural earthquakes: search for a seismic descriminant, submitted to the Bull. Seis. Soc. Am.

Priestley, K., and J. Brune (1978). Surface waves and the structure of the Great Basin of Nevada and western Utah, J. Geophys. Rev., 83, 2265.

Priestley, K., J. Brune, and J. Orcutte (1979). Higher mode surface waves and structure of the Great Basin of Nevada and western Utah, to be submitted to J. Geophys. Res.

Ryall, A., and A. E. Jones (1964). Computer programs for automatic processing of Basin and Range seismic data, Bull. Seis. Soc. Am., 54, 2295.

Ryall, A., and D. J. Stuart (1963). Travel-times and amplitudes from nuclear explosions, Nevada test site to Ordway, Colorado, J. Geophys. Rev., 68, 5821.

Sass, J. H., W. H. Diment, A. H. Lachenbruch, B. V. Marshall, R. J. Munroe, T. H. Mosses, Jr., and T. C. Urban (1976). A new heat flow contour map of the Conterminous United States, U.S.G.S. Open File Rept., 76, 756.

Smith, R. (1977). Intraplate tectonics of the western North American plate, Tectonophysics, 37, 323.

Stauber, D. A., and D. M. Bovre (1978). Crustal thickness in northern Nevada from seismic refraction profiles, Bull. Seis. Soc. Am., 68, 1049.

Stewart, J. H., and J. E. Carlson (1976). Cenozoic rocks of Nevada, map 52, Nev. Bur. of Mines and Geol., Univ. of Nev., Reno.

Suppe, J., C. Powell, and R. Berry (1975). Regional topography, seismicity, Quaternary volcanism, and the present-day tectonics of western United States, Am. J. Sci., 275-A, 397.

Willmon, P. L., and A. M. Bancroft (1960). The time-term approach to refraction seismology, Geophys. Jour., 3, 419.

TABLE 1. Epicentral Information for Earthquakes Analyzed in This Study

Date	Origin Time	Latitude	Longitude	Nuclear Event
Jan. 6, 1975	11h17m12.3s	35.931N	120.534W	
Mar. 28, 1975	02h31m05.75	42.061N	112.548W	
Jun. 3, 1975	14h20m00.170s	37.340N	116.522W	Stilton
Jun. 3, 1975	14h40m00.106s	37.094N	116.034W	Mizzon
Jun. 19, 1975	13h00m00.090s	37.350N	116.320W	Mast
Jun. 26, 1975	12h30m00.161s	37.279N	116.369W	Camembert
Aug. 1, 1975	20h20m12.9s	39.439N	121.528W	
Aug. 31, 1975	11h27m39.7s	40.950N	119.113W	
Sep. 6, 1975	17h00m00.113s	37.023N	116.028W	Marsh
Sep. 26, 1975	02h31m6.8s	39.490N	121.573W	
Sep. 27, 1975	22h34m38.1s	39.512N	121.537W	
Oct. 24, 1975	17h11m26.096s	32.221N	116.179W	Husky Pup
Oct. 28, 1975	14h30m00.160s	37.290N	116.411W	Kasseri
Nov. 15, 1975	03h35m1.6s	39.417N	121.572W	
Nov. 20, 1975	15h00m00.093s	37.224N	116.367W	Inlet
Dec. 20, 1975	20h60m00.164s	37.226N	116.165W	Chiberta
Feb. 4, 1976	14h20m00.112s	37.092N	116.151W	Kalon
Feb. 4, 1976	14h40m00.163s	37.165N	116.074W	Lsrom
Feb. 12, 1976	14h45m00.163s	37.314N	116.534W	Fontina
Feb. 14, 1976	11h30m00.162s	37.326N	116.452W	Cheshire
Mar. 9, 1976	14h00m00.094s	37.399N	116.492W	Estuary
Mar. 14, 1976	12h30m00.163s	37.359N	116.514W	Colby
Mar. 17, 1976	14h15m00.092s	37.308N	116.435W	Pool
Mar. 17, 1976	14h45m00.091s	37.172N	116.074W	Strait
May 12, 1976	19h50m00.170s	37.290N	116.234W	Might Epic
Jun. 20, 1976	10h15m24.0s	40.394N	120.518W	
Jun. 24, 1976	15h44m44.3s	40.418N	120.578W	
Jul. 6, 1976	03h55m16.2s	39.399N	121.601W	
Jul. 27, 1976	20h30m00.079s	37.153N	116.138W	Billet
Aug. 22, 1976	10h14m6.5s	38.910N	116.430W	
Nov. 23, 1976	15h15m00.163s	37.217N	116.076W	Levre
Dec. 21, 1976	15h09m00.166s	37.189N	116.074W	Asiago
Dec. 28, 1976	18h00m00.076s	37.104N	116.074W	Rupper
Apr. 5, 1977	14h00m00166s	37.153N	116.172W	Marksilly
Apr. 27, 1977	15h00m00.084s	37.197N	116.128W	Bulkhead
May 25, 1977	17h00m00.076s	37.193N	116.148W	Crewline
Aug. 4, 1977	16h40m00.074s	37.115N	116.068W	Strake
Aug. 19, 1977	17h55m00.075s	37.200N	116.095W	Scantling
Sep. 15, 1977	14h36m30.1s	37.003N	116.043W	Ebb Tide
Sep. 27, 1977	14h00m00.2s	37.151N	116.068W	Coulmmiers
Oct. 26, 1977	14h15m00.1s	37.008N	116.017W	Bobstay
Nov. 1, 1977	18h06m00.1s	37.188N	116.213W	Hybla Gold
Nov. 9, 1977	22h00m00.1s	37.072N	116.050W	Sandreef
Nov. 17, 1977	19h30m00.1s	37.021N	116.025W	Seamount
Dec. 14, 1977	15h30m00.2s	37.136N	116.086W	Farallones
Feb. 23, 1978	14h00m00.161s	37.124N	116.064W	
Mar. 23, 1978	16h30m00.000s	37.099N	116.020W	
Apr. 11, 1978	15h30m00.073s	37.299N	116.326W	
Apr. 11, 1978	17h45m00.161s	37.233N	116.368W	

Date	Origin Time	Latitude	Longitude	Nuclear Event
May 23, 1978	05h47m55.8s	40.890N	117.310W	
Jul. 6, 1978	22h21m21.8s	39.090N	116.220W	
Jul. 12, 1978	17h00m00.0s	37.078N	116.044W	Lowball
Aug. 1, 1978	09h02m34.5s	41.457N	121.870W	
Aug. 13, 1978	22h54m53.5s	34.350N	119.700W	
Aug. 31, 1978	14h00m00.0s	37.276N	116.358W	Panir
Sep. 8, 1978	16h59m46.0s	38.668N	121.905W	
Sep. 13, 1978	15h15m00.2s	37.210N	116.210W	Diab lo Hawk
Nov. 2, 1978	15h25m00.0s	37.288N	116.110W	Emmenthal

TABLE 2. WESTERN GREAT BASIN COMPRESSIONAL WAVE VELOCITIES

Crustal velocity	
Average phase velocity from local earthquakes	6.08 K/S
$\overline{P}$ velocity	6.25 K/S
Upper Mantle velocity	
Average phase velocity from regional earthquakes and explosions	7.81 K/S
Time-term method velocity determination	7.77 K/S
Pn residual correction method velocity determination	7.85 K/S
Average reversed-refraction velocity	7.82 K/S
Upper Mantle velocity vs. period for same path	
1.0 ± 0.5 seconds period	7.75 K/S
3.5 ± 0.2 seconds period	7.90 K/S
9.8 ± 0.3 seconds period	8.01 K/S

FIGURE CAPTIONS

Figure 1. Location map showing relationship of refraction profile of this study (bold lines) with previous refraction studies in the northern Basin and Range. Insert shows details of the seismograph locations in the western Great Basin.

Figure 2. Travel-time curves for the (a) Hawthorne profile and (b) Tonopah profile.

Figure 3. Record section for the Tonopah profile. Data collected with smoke-paper recorders are indicated only by arrival times.

Figure 4. Comparison of Tonopah profile data: (a) reducted travel-time data; (b) equivalent crustal thickness; (c) free-air gravity; (d) Bouguer gravity; (e) elevation; (f) computed Bouguer gravity.

Figure 5. Comparison of data for western Great Basin: (a) relative Pn residuals; (b) equivalent crustal thickness; (c) free-air gravity; (d) Bouguer gravity.

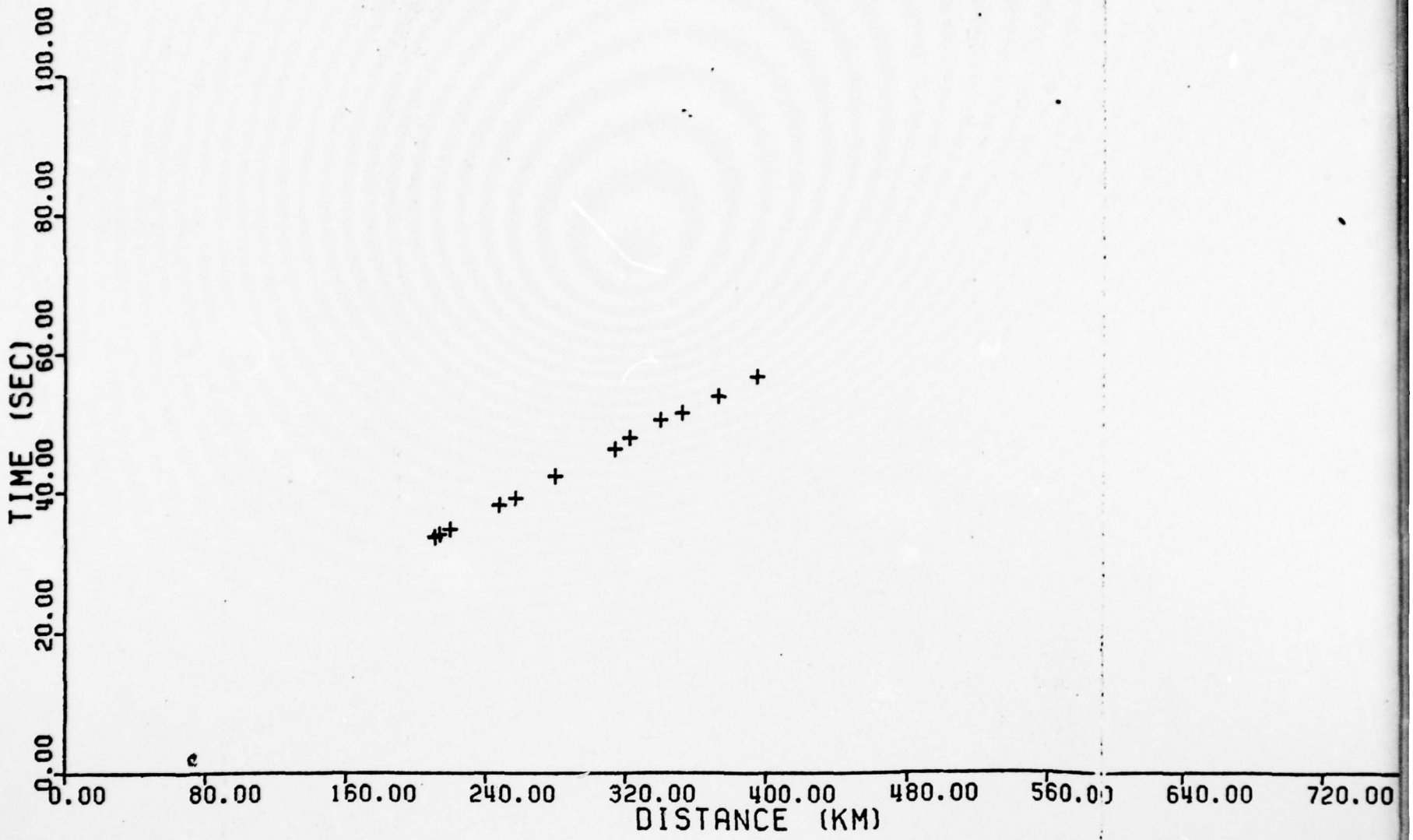
TIME (SEC)
0.00
20.00
40.00
60.00
80.00
100.00
0.00
80.00
160.00
240.00
320.00
400.00
480.00
560.00
640.00
720.00
DISTANCE (KM)

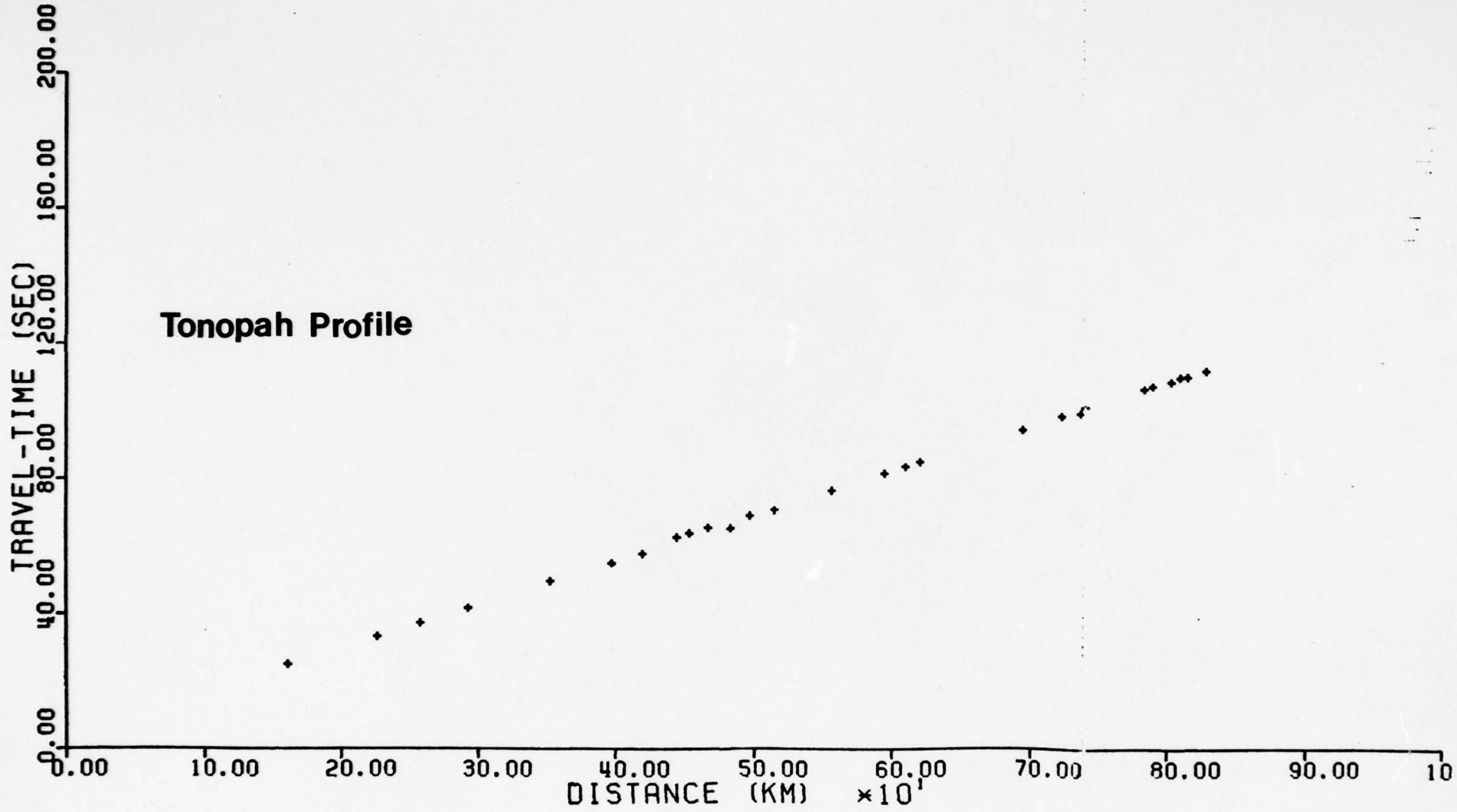
Tonopah Profile
TRAVEL-TIME (SEC)
0.00
40.00
80.00
120.00
160.00
200.00
0.00
10.00
20.00
30.00
40.00
50.00
60.00
70.00
80.00
90.00
DISTANCE (KM) ×10¹

Time in seconds
0
Distance in Kms.

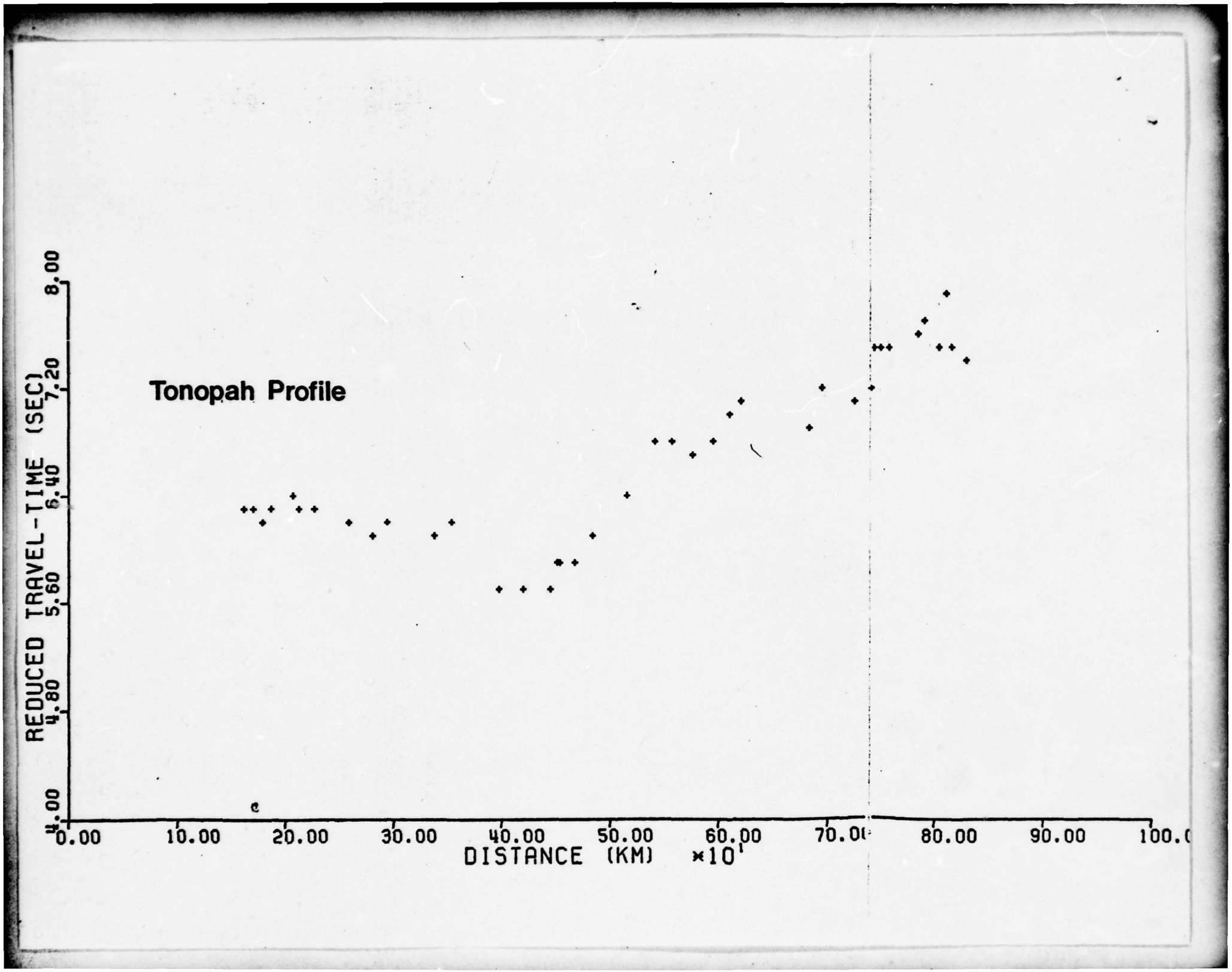
Tonopah Profile
REDUCED TRAVEL-TIME (SEC)
4.00
4.80
5.60
6.40
7.20
8.00
0.00
10.00
20.00
30.00
40.00
50.00
60.00
70.00
80.00
90.00
100.0
DISTANCE (KM) ×10¹

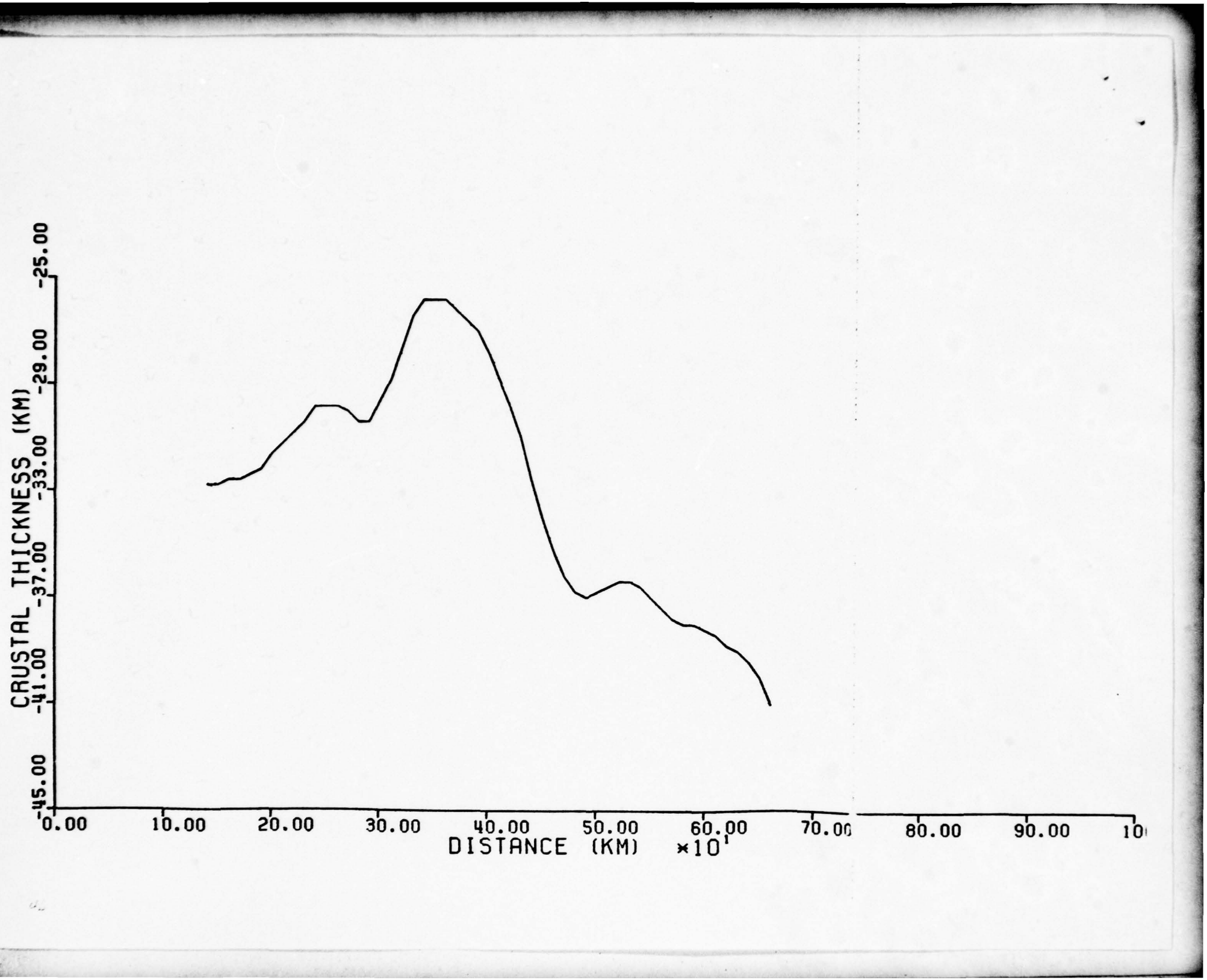
CRUSTAL THICKNESS (KM)
-25.00
-29.00
-33.00
-37.00
-41.00
-45.00
0.00
10.00
20.00
30.00
40.00
50.00
60.00
70.00
80.00
90.00
DISTANCE (KM) ×10¹

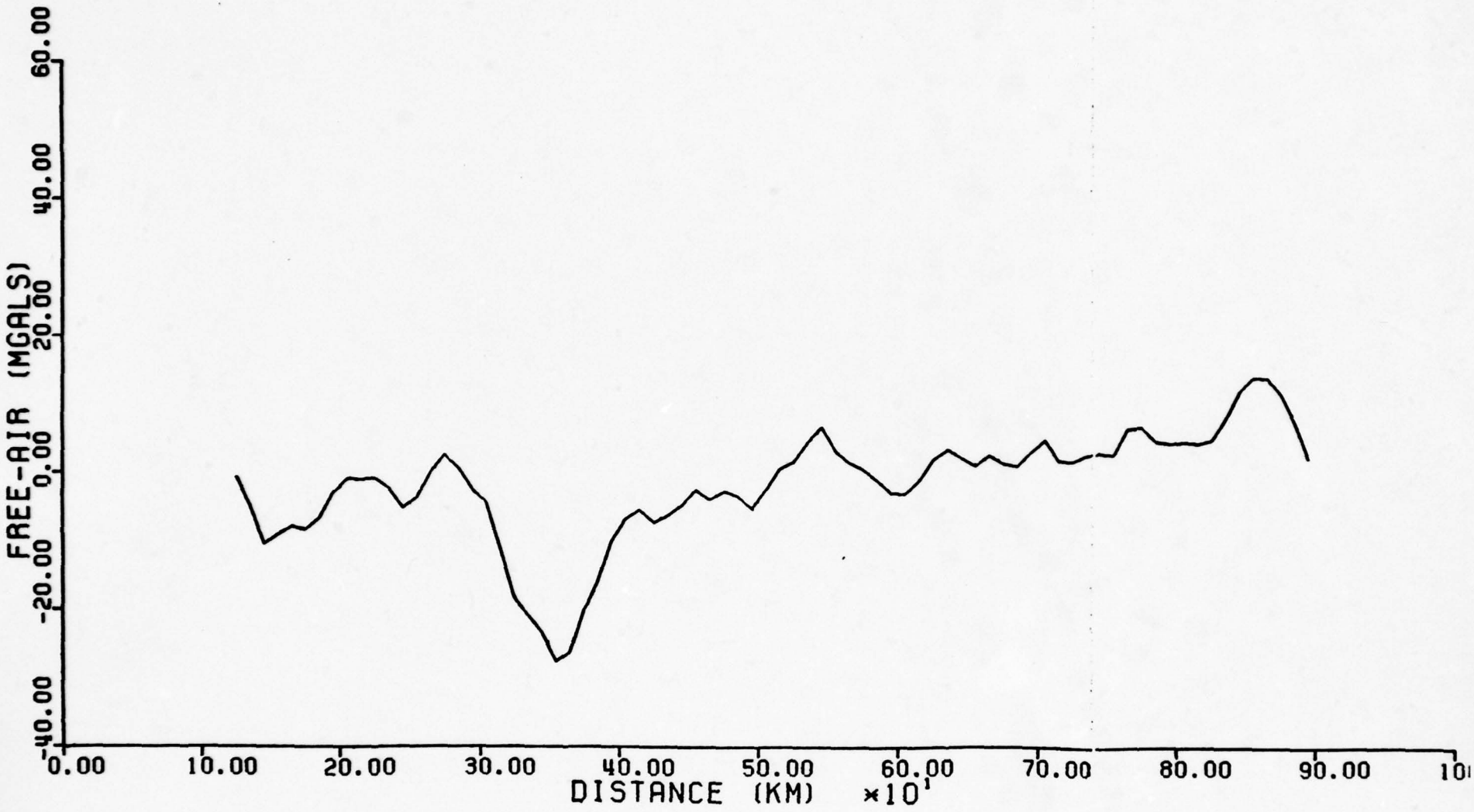
FREE-AIR (MGALS)
60.00
40.00
20.00
0.00
-20.00
-40.00
0.00
10.00
20.00
30.00
40.00
50.00
60.00
70.00
80.00
90.00
DISTANCE (KM) ×10¹

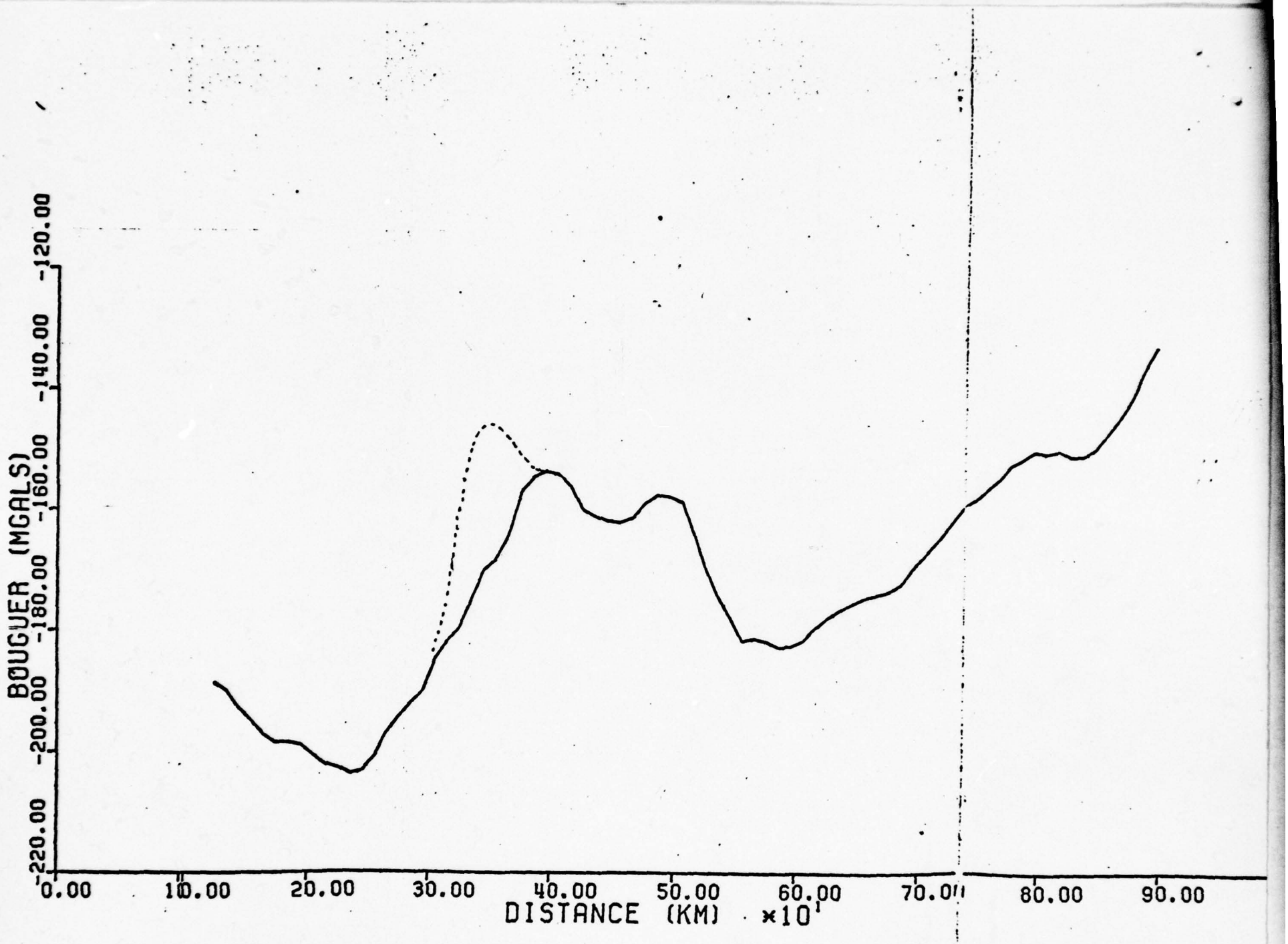
BOUGUER (MGALS)
-120.00
-140.00
-160.00
-180.00
-200.00
-220.00
0.00
10.00
20.00
30.00
40.00
50.00
60.00
70.00
80.00
90.00
DISTANCE (KM) ×10¹

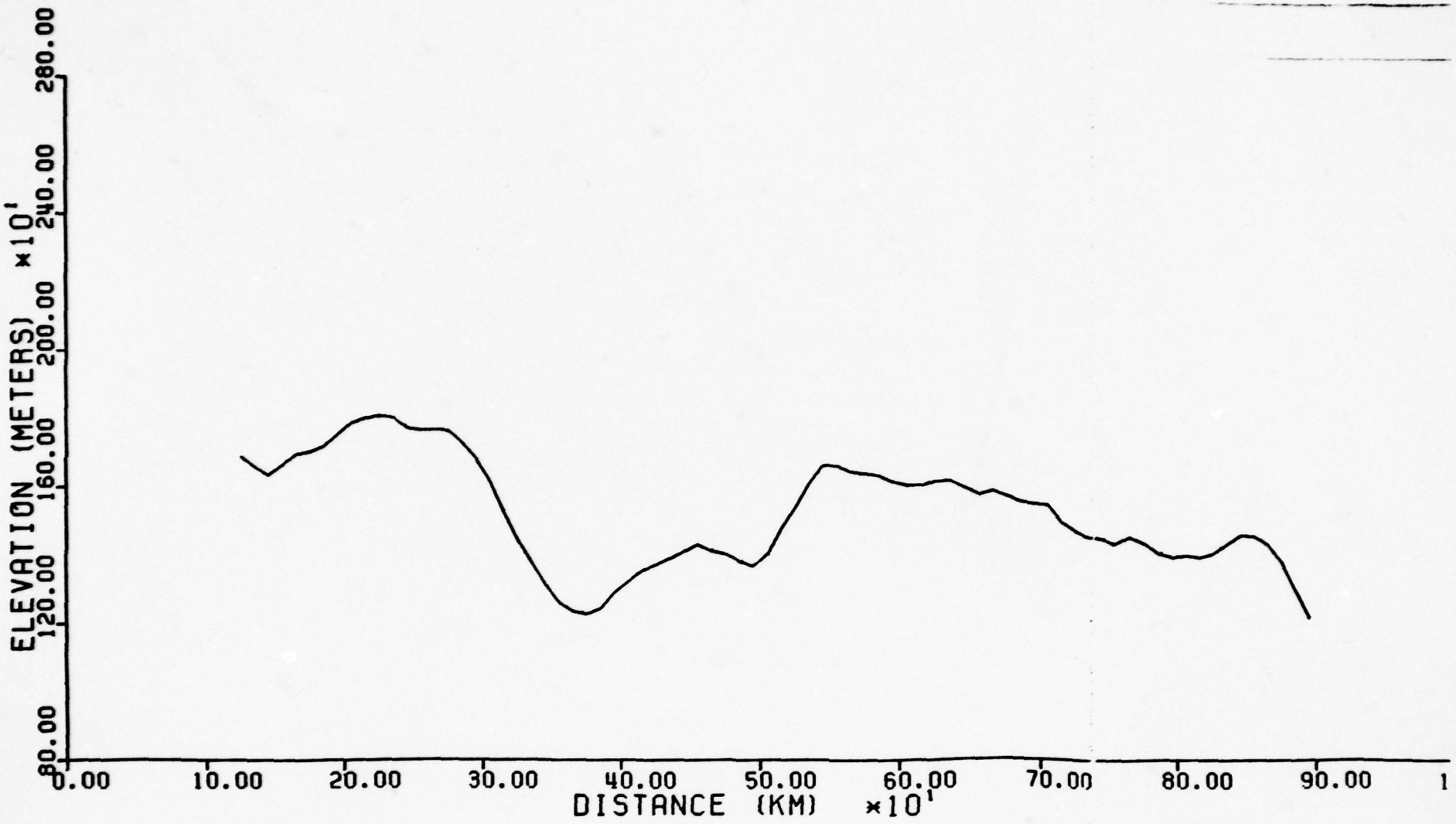
ELEVATION (METERS) ×10¹
280.00
240.00
200.00
160.00
120.00
80.00
0.00
10.00
20.00
30.00
40.00
50.00
60.00
70.00
80.00
90.00
1
DISTANCE (KM) ×10¹

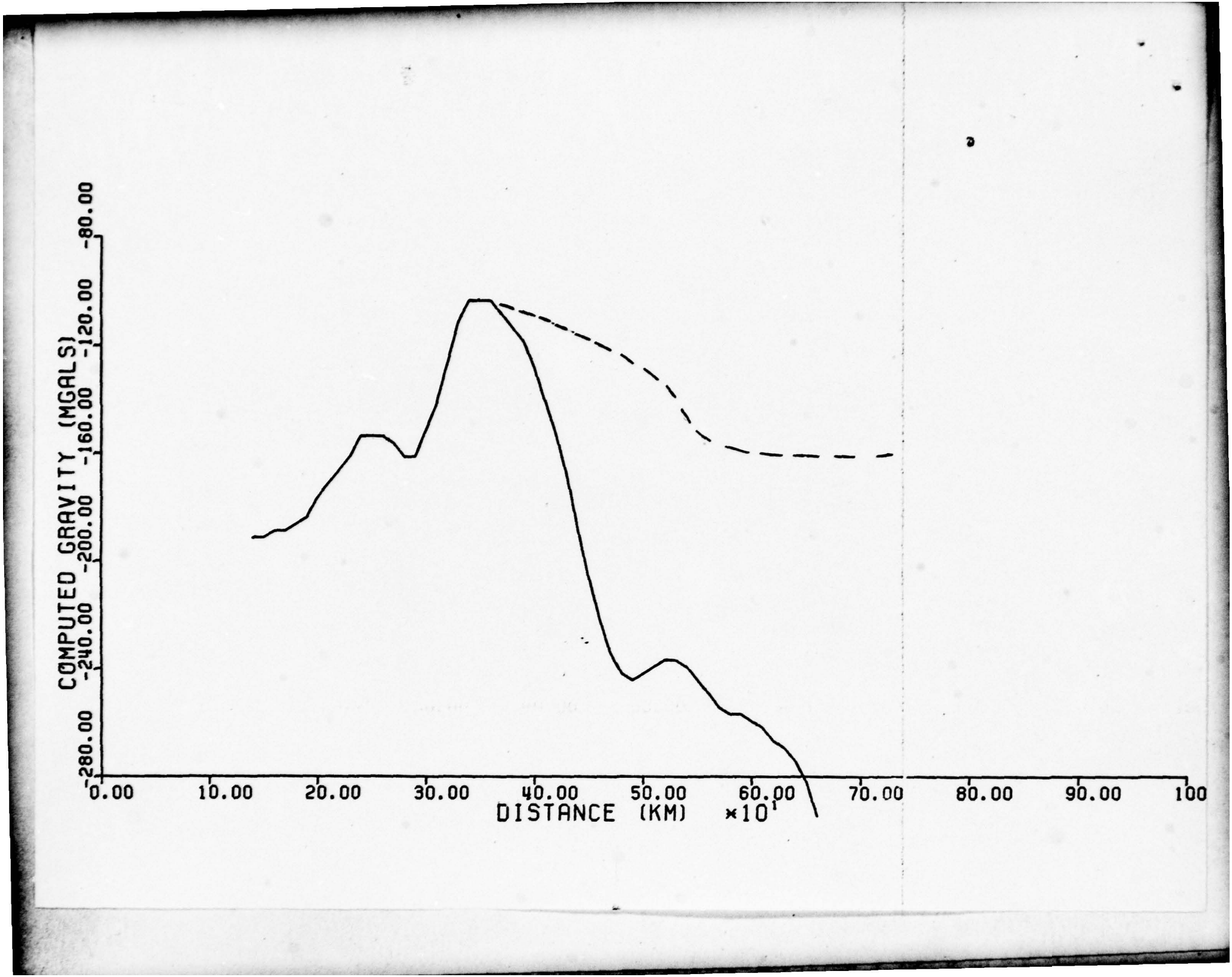
COMPUTED GRAVITY (MGALS)
-80.00
-120.00
-160.00
-200.00
-240.00
-280.00
0.00
10.00
20.00
30.00
40.00
50.00
60.00
70.00
80.00
90.00
100
DISTANCE (KM) ×10¹

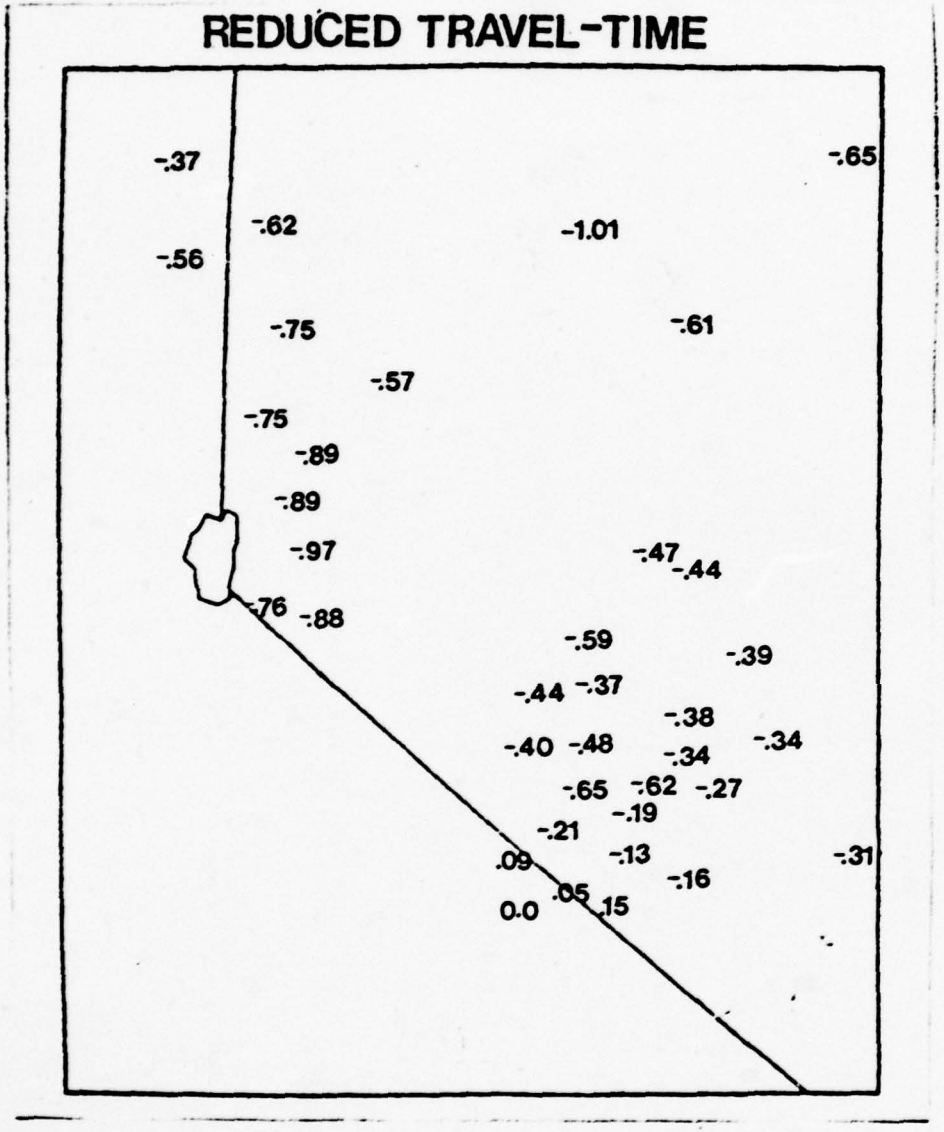
REDUCED TRAVEL-TIME
-.37
-.65
-.62
-1.01
-.56
-.75
-.61
-.57
-.75
-.89
-.89
-.97
-.47
-.44
-.76
-.88
-.59
-.39
-.44
-.37
-.38
-.40
-.48
-.34
-.34
-.65
-.62
-.27
-.19
-.21
-.13
-.31
.09
-.16
.05
.15
0.0

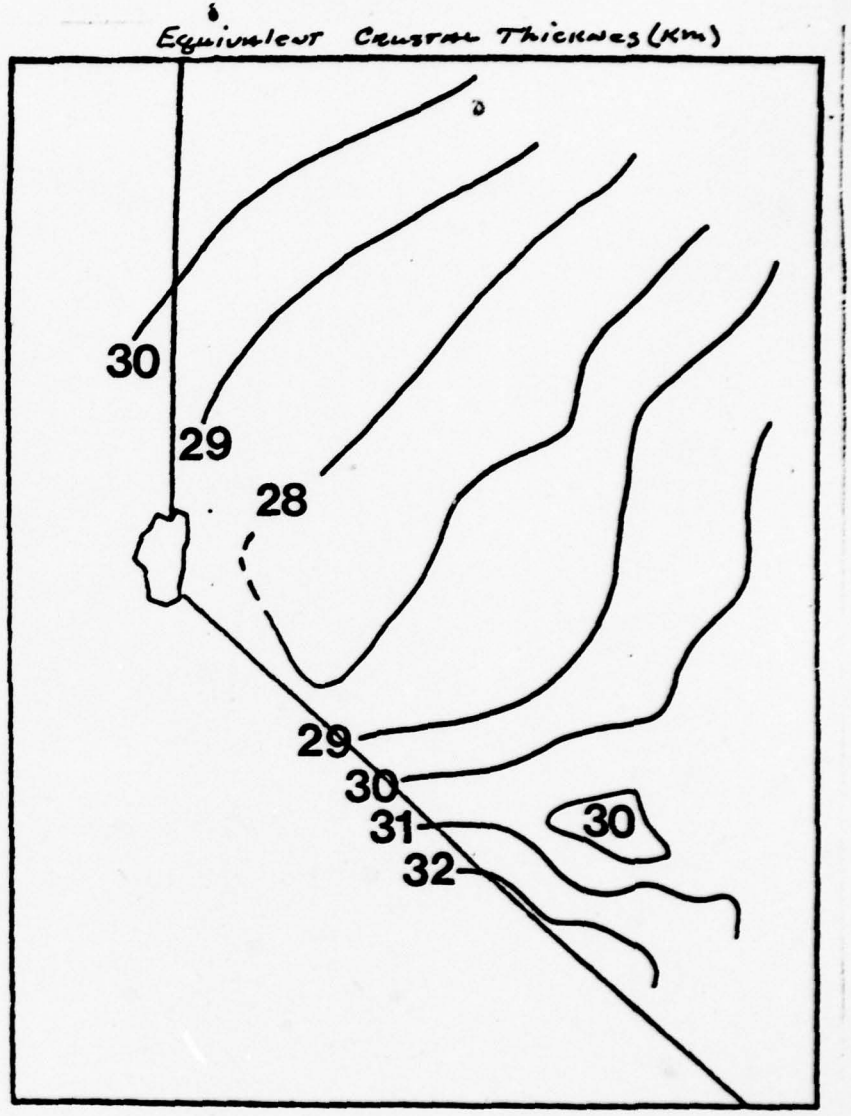
Equivalent Crustal Thickness (Km)
30
29
28
29
30
31
32
30

FREE-AIR GRAVITY

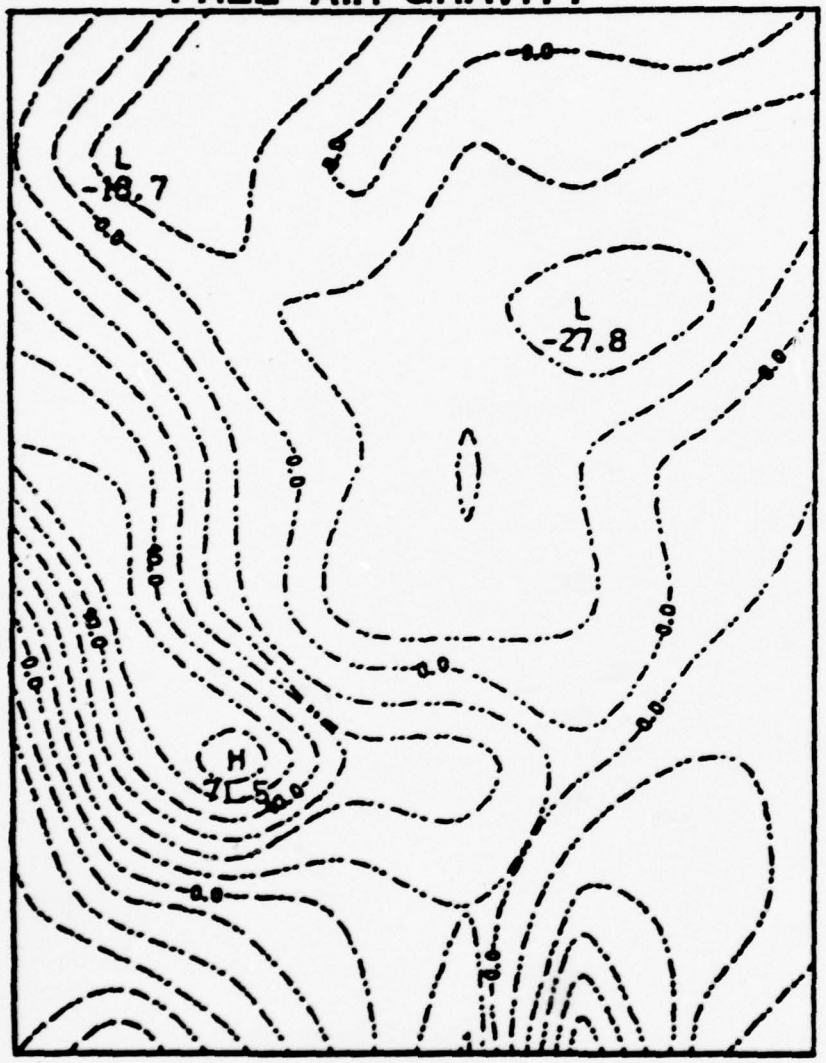

BOUGUER GRAVITY

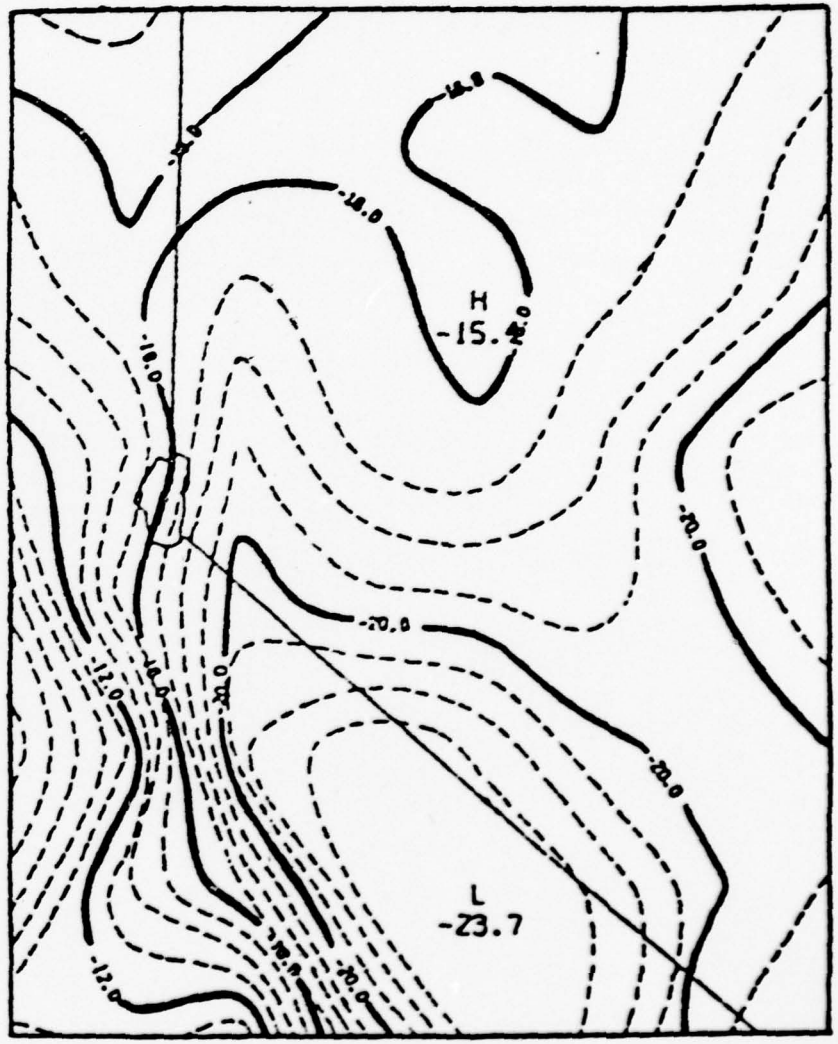

Appendix B

Higher Mode Surface Wave and Structure of the Great Basin of Nevada and Western Utah

Keith Priestley
Seismological Laboratory, Mackay School of Mines
University of Nevada, Reno, Nevada 89557

James Brune
Institute of Geophysics and Planetary Physics,
Scripps Institution of Oceanography
University of California, San Diego, La Jolla, California 92037

John Orcutte
Geological Research Division
Scripps Institution of Oceanography
University of California, San Diego, La Jolla, California, 92037

Abstract

Observed seismograms and phase and group velocity data for crust and mantle higher mode surface waves in the Great Basin are compared with theoretical seismograms and dispersion curves computed for the GREAT BASIN model derived from fundamental mode data by Priestley and Brune (1978). Phases identified as Sa or long period Sn ($T \simeq 13$ sec.) are observed to have a phase velocity of $4.50 \pm .03$ km/sec. Crustal 2nd Rayleigh mode (first shear mode) waves have predominant periods varying from about 5 seconds on some paths to about 8 seconds on others.

The observed excitation and phase velocity of the Sa phase are in agreement with theoretical seismograms and computed phase velocities for the GREAT BASIN model. The agreement provides added support for the existence of a mantle lid of velocity about 4.5 km/sec. and thickness about 30 km in the Great Basin.

The crustal higher mode group velocity observations, i.e., the predominant periods of the 2nd Rayleigh mode along various paths reflect variations in crustal thickness within the Great Basin. Crustal thicknesses of approximately 20 km are indicated for some paths in northwestern Nevada and southeastern Oregon whereas crustal thicknesses of greater than 35 km are indicated for east-central Nevada. The crustal thickness of 35 km in the GREAT BASIN model is probably appropriate for the central part of the Great Basin.

Introduction

In a previous paper (Priestley and Brune, 1978) fundamental mode surface wave dispersion was measured for a number of paths in the Great Basin of Nevada and western Utah. Using this data and existing refraction data, an average structural model was derived for the Great Basin. This model, referred to as the GREAT BASIN model has a 3 layer crust of thickness 35 km, an upper mantle lid of shear velocity 4.5 km/sec and thickness 29 km, and an extreme low velocity layer of shear velocity about 4.1 km/sec and thickness about 120 km (Table 1). The pronounced low velocity zone in this model is similar to that found by Knopoff et al. (1970) for an oceanic rise structure, and by Knopoff and Schlue (1972) for the East African Rift. This result supports the conclusion that the Great Basin is a zone of rifting.

Some of the questions that naturally arise concerning the Priestley and Brune (1978) study are:

1. How much variation in crustal thickness occurs within the Great Basin? Some evidence for such variations, based on observed fundamental mode surface wave dispersion was discussed by Priestley and Brune (1978).
2. How certain is the existence and proposed 30 km thickness of the upper mantle lid of shear velocity 4.5 km/sec? This is an interesting question because of suggestions that in zones of rifting, the low velocity zone may extend to the crust and thus a lid over the low velocity zone, typically found in more stable areas, might not be present.

To help answer these questions we have searched for higher mode surface wave data which might provide independent evidence concerning the structure of the Great Basin. For certain aspects of earth structure higher mode data can often provide better resolution than fundamental mode data.

1. We have observed the propagation of the Sa phase (long period Sn) between the stations Reno and Tonopah from earthquakes off the coast of Oregon and

Washington. Since this phase is travelling in the upper mantle lid (analogous to Sn) its velocity should provide a constraint on the lid velocity and its wavelength a constraint on the lid thickness.

2. We have observed 2nd Rayleigh mode (1st shear mode waves) along a number of paths within the Great Basin. This mode has a steep group velocity curve near the period of crustal resonance. The period of this steep part of the curve is readily measured and is directly proportional to the crustal thickness (Oliver and Ewing, 1958). Thus it can be used as a straightforward method of determining average crustal thickness over a given path and of observing variations in crustal thickness from path to path.

DATA

Figure 1 shows the location of the earthquakes analyzed and the paths studied.

Sa: We have observed a very clear Sa phase at REN and TNP from earthquakes off the coast of Oregon and Washington. The Sa phase is analogous to Sn except that it is lower frequency and must be considered as a normal mode or superposition of normal modes rather than as a ray or head wave. The name was given by Caloi (1954) who applied it to a conspicuous pulse of longer period (20-30 sec) often seen at teleseismic distances. Brune (1965), Schwab, et al. (1974) and others have interpreted it as a guided wave corresponding as a superposition of normal modes. We will discuss its interpretation further in a later section.

Since the epicenters of the earthquakes used are nearly in line with the stations REN and TNP, we have been able to measure the phase velocity of its predominant period by phase correlation between REN and TNP. Figure 2 shows examples of this phase. It has a predominant period of about 13 seconds (range from about 12-15 sec) and an arrival time corresponding approximately to the

arrival time expected for Sn. Its group arrival time corresponds to a group velocity between roughly 4.0 and 4.5 km/sec. Because it consists of a group of relatively long period energy, its group velocity cannot be determined as accurately as its phase velocity.

The estimated phase velocity at a period of 13 sec from 4 observations is $4.5 \pm .03$ km/sec. This result will be compared with theoretical computations in a later section.

2nd Rayleigh Mode: The second Rayleigh mode is commonly observed on long period vertical seismograms as a train of waves of relatively slowly varying periods extending from near the expected S-wave arrival time up to the arrival of the long period fundamental mode Rayleigh wave. Examples of second Rayleigh mode data used in this study are shown in Figure 3. Because the period changes so slowly with time (i.e., the dispersion is so great) it is often difficult to determine the slope of the group velocity very accurately. However, for the same reason, the period of the waves can be determined quite accurately. Theoretical calculations show that the predominant period of the steep portion of the group velocity curve is directly proportional to average crustal thickness (Oliver and Ewing, 1958) and hence is very useful in determining average crustal thickness.

We have measured the predominant period of the crustal 2nd Rayleigh mode for a number of paths in the Great Basin. The results are presented in Table 3. In some cases we were able to approximately estimate the slope of the dispersion curve (i.e., we could observe definite dispersions in the wave train) and in these cases we have indicated a range in velocities and periods. The results will be compared with theoretical calculations in a later section.

THEORETICAL CALCULATIONS

To interpret the data presented above, we have made two types of calculations using the GREAT BASIN model. First, we have compiled theoretical seismograms using a direct wave number integration program developed by Apsel and Luco (unpublished). Second, we have computed phase velocity, group velocity and particle motion diagrams using the normal mode program of Harkrider (1964, 1970).

Theoretical Seismograms: Using the Apsel and Luco direct wave number integration program we have calculated theoretical seismograms for the GREAT BASIN model without the low velocity surface layer, over a range of distances to illustrate the character of the theoretical seismograms. The low velocity surface layers were removed because the recording stations are sited on bedrock. In computing the theoretical seismograms we have assumed a double couple point source at a depth of 10 km, corrected for Q assuming a value of 300 and corrected for instrument response for a Press-Ewing 15-90 long period seismograph. These results are presented in Figure 4. The theoretical seismograms are remarkably similar to the observed seismograms (Figures 2 and 3) indicating that the GREAT BASIN model corresponds closely to the earth structure of this region. It should be noted that the Sa phase and crustal higher mode are clearly shown and have approximately the same character as the observed seismograms.

The period and phase velocity of the Sa phase can be determined directly from the theoretical seismograms using the same technique as for the observed data. The predominant period and phase velocity of the Sa phase on the theoretical seismogram is 13 seconds and 4.51 km/sec respectively, in excellent agreement with the period and phase velocity of the observed Sa phases.

The predominant period of the crustal second Rayleigh mode is directly proportional to crustal thickness. The GREAT BASIN model has a 35 km thick crust and the predominant period of the crustal second Rayleigh mode is 7 to 8 seconds.

We may approximately determine the average crustal thickness for the observed paths by directly comparing the observed and theoretical predominant period of the crustal second Rayleigh mode. Thus we obtain the estimated crustal thickness listed in the third column of Table 3.

The results of the above theoretical seismogram computation provide strong support for the GREAT BASIN model determined previously from fundamental mode Rayleigh wave and Love wave dispersion. In particular the agreement between the theoretical and observed Sa phase strongly supports existence of a 4.5 km/sec velocity, 30 km thick mantle lid over the low velocity zone.

Theoretical Dispersion Curves and Particle Motion Diagrams: To identify the particular higher modes contributing to the observed data, we have computed higher mode phase velocity, group velocity and particle motion diagrams for the GREAT BASIN model derived from the fundamental mode surface wave data. To calculate these curves we have used the normal mode computer program of Harkrider (1964, 1970).

The observed Sa phase consists of energy propagating with a predominant period of 13 sec. and with a phase velocity of 4.5 k/s. This pulse is composed of a number of higher mode covering a range of frequencies and propagating with phase velocity near 4.5 k/s. However, from the higher mode Rayleigh wave phase velocity curves (Figure 5) it can be seen that the observed phase is primarily composed of energy of the third higher Rayleigh mode. Figure 6 is the energy density plot for the third higher Rayleigh mode at 12.25 seconds period and phase velocity 4.54 k/s. Peaks in the energy distribution occur in the mantle lid, within the low velocity zone, and in the 4.5 k/s layer at the base of the low velocity zone. This mode of propagation is analogous to two rays propagating in the 4.5 k/s layers with the third ray in the low velocity zone resulting from constructive interference of the shallow and deep ray. The energy propagating in the mantle lid is trapped within the 4.5 k/s layer due to the natural velocity

gradient created by the earth's sphericity. This is analogous to the findings of Stephens and Issack (1977) for short period Sn.

Figure 7 is the higher Rayleigh mode group velocity curves computed for the fundamental mode GREAT BASIN model. The observed data for the crustal second Rayleigh mode is indicated by the short, heavy line segments. The steep portion of the group velocity curve is extremely sensitive to the average crustal thickness along the path of propagation (Oliver and Ewing, 1958). The relationship between the observed and theoretical period of the steep portion of the group velocity curve can be linearly related to variations in actual crustal thickness compared with that of the GREAT BASIN model. The crustal second Rayleigh mode data, as pointed out previously, indicates considerable variation in crustal thickness within the northern Basin and Range.

DISCUSSION

In this paper we have presented higher mode surface wave observations within the northern Basin and Range, and have interpreted them in terms of the GREAT BASIN model of Priestley and Brune (1978). These results are summarized in Figure 8.

The Sa phase or long-period Sn phase which is observed to propagate along the path REN-TNP, is interpreted as being composed primarily of the third higher Rayleigh mode. The characteristics of this phase arise from energy being trapped in the mantle lid as the result of the natural velocity gradient created by sphericity. The observed phase velocity of 4.5 k/s confirms the 4.5 k/s shear wave velocity of the mantle lid for the fundamental mode model. The Sa phase propagates across the western Great Basin with little attenuation, indicating that the thickness of the mantle lid is comparable to the wavelength of the Sa phase. The predominant period is 13 seconds corresponding to a half wavelength of 29 km, in reasonable agreement with the mantle lid thickness determined from

the fundamental mode data. If the lid thickness was significantly less than this, the Sa pulse would be rapidly attenuated due to the leakage of energy into the low velocity zone.

Clear second Rayleigh modes have been observed at long period seismic stations in the Great Basin for earthquakes within the northern Basin and Range. This mode has a steep group velocity curve near the period of crustal resonance and thus the period of phase can be accurately determined and is sensitive to the average crustal thickness along the path of propagation. The period of this phase varies from 5 to 8 seconds, indicating a significant variation in crustal thickness within the Great Basin. The crustal structure of the GREAT BASIN model determined by Priestley and Brune (1978) was constrained by compressional wave travel-time data, and fundamental mode Rayleigh wave and Love wave dispersion data. The available refraction data (Eaton, 1963; Ryall and Stuart, 1963; Johnson, 1965; Hill and Pakiser, 1967; unpublished University of Nevada data) was averaged to produce a representative set of travel-time curves for the Great Basin. This set of travel-time curves indicated the average crustal thickness of the Great Basin was 35 km and was composed of three layers: a sedimentary layer (H=2.5 km, Vp=3.55 k/s), a granitic layer (H=22.5 km, Vp=6.10 k/s) and an intermediate layer (H=10 km, Vp=6.6 k/s). The average Pn velocity was 7.8 k/s. An excellent fit of the surface wave data was obtained by assuming a poisson's ratio of .25 and setting the shear wave velocities to 2.05 k/s, 3.55 k/s and 3.85 k/s respectively in the sedimentary, granitic and intermediate crustal layers. The upper mantle shear wave velocity was determined to be 4.50 k/s.

The variations in predominant period of the crustal higher mode implies significant variations in crustal thickness within the Great Basin. Five of the paths for which crustal higher modes were observed cross the Battle Mountain heat flow high (Sass, et al., 1976), an area of high continental heat flow trending northeastwards from the vicinity of Reno across the northern Great Basin.

The period of crustal resonance for the Idaho-Reno path corresponds to a crustal thickness of 37 km. This path crosses the Battle Mountain high but includes a large section of path in the Snake River Plain and Oregon Volcanic Province. The Adel-Dugway and Adel-Tonopah paths (29.5 km and 31 km average crustal thickness, respectively) cross the Battle Mountain high but include portions of the volcanic province and areas of more normal Great Basin heat flow. The two remaining paths in the northern Great Basin, Adel-Reno and Winnemucca-Dugway (both 23 km average crustal thickness), are nearly confined to the region of high heat flow. This crustal thinning within the Battle Mountain heat flow indicated by the higher mode data is supported by travel-time data from Nevada Test Site explosions through the same area (Stauber and Boore, 1978; Priestley and Fezie, 1979).

SUMMARY

1. Higher mode surface wave observations within the Great Basin of Nevada and western Utah have been presented. These consist of a Sa or long-period Sn phase observed for a number of earthquakes located off the coast of Oregon and Washington and crustal higher modes for moderate earthquakes located within the Great Basin.

2. The Sa phase has been identified as consisting primarily of the third higher Rayleigh mode and propagating with a significant energy content within the mantle lid. The energy is trapped within the lid by the natural positive velocity gradient resulting from the earth's sphericity. The 4.50 ± 0.03 k/s phase velocity of the Sa phase is in excellent agreement with the 4.50 k/s shear wave velocity of the lid determined from fundamental mode dispersion data. The 13 ± 2 sec predominant period of the Sa phase corresponds to wavelengths comparable to the thickness of the lid determined from the fundamental mode data. Thus this higher mode data provides strong support for the existence of the relatively thick mantle lid of the GREAT BASIN model.

3. The crustal higher mode data indicates there are significant variations in the crustal thickness within the Great Basin. The fundamental mode data indicates an average crustal thickness of 35 km. However, across the northern Great Basin, the area of the Battle Mountain heat flow high, the crust is as thin as 23 km.

ACKNOWLEDGMENTS

This research has been supported in part by the Advanced Research Project Agency and was monitored by the Air Force Office of Scientific Research under contract F49620-77-C-0070, by the National Science Foundation under grant EAR77-13625, and by the U. S. Geological Survey under grant 14-08-0001-G-433.

REFERENCES

Brune, J., The Sa phase from the Hindu Kush Earthquake of July 6, 1962, Pure Appl. Geophys., 62, p. 81, 1965.

Caloi, P., L'Astenostera Comi Canch-guidi dell' energia sismica, Annali di Geofisica, 7, 1954.

Eaton, J. P., Crustal structure from San Francisco, California, to Eureka Nevada, from seismic refraction measurements, Jour. Geophys. Res., 68, p. 5789, 1963.

Harkrider, P. G., Surface waves in multilayered elastic media. Part I. Rayleigh and Love Waves from buried sources in a multilayered elastic half-space, Bull. Seism. Soc. Am. 54, p. 627, 1964.

Harkrider, P. G., Surface waves in multilayered elastic media. Part II. Higher mode spectra and spectral ratios from point sources in plain layered earth models, Bull. Seism. Soc. Am., 60, p. 1937, 1970.

Johnson, L. R., Crustal structure between Lake Mead, Nevad and Mono Lake, California, Jour. Geophys. Res., 70, p. 2863, 1965.

Knopoff, L., J. Schlue, and F. A. Schwab, Phase velocities of Rayleigh waves across the East Pacific Rise, Tectonophysics, 10, p. 321, 1970.

Knopoff, L., and J. Schlue, Rayleigh wave phase velocities for the path Addis Ababa-Nairobi, Tectonophysics, 15, p. 157, 1972.

Oliver, J. and M. Ewing, Normal modes of Continental surface waves, Bull. Seismo. Soc. Am., 48, p. 33, 1958.

Pakiser, L. C., and D. P. Hill, Seismic refraction study of crustal structure between the Nevada Test Site and Boise, Idaho, Geol. Soc. Am. Bull. 78, p. 685, 1967.

Priestley, K., and J. Brune, Surface waves and the structure of the Great Basin of Nevada and Western Utah, Jour. Geophys. Res., 83, p. 2265, 1978.

Priestley, K. and G. Fezie, Crustal structure from Tonopah, Nevada to Bend, Oregon from seismic refraction measurements, to be submitted to Bull. Seism. Soc. Am.

Ryall, A., and D. J. Stuart, Travel-times and amplitudes from nuclear Explosions, Nevada Test Site to Ordway, Colorado, Jour. Geophys. Res., 68, p. 5821.

Sass, J. H., W. H. Diment, A. H. Lackenbruch, B. V. Marshall, R. J. Munroe, T. H. Morse, Jr., and T. C. Urban, A new heat flwo contour map of the conterminous United States, U.S.Geol. Survey Open-File Rept. 76, p. 756, 1976.

Schwab, F., Kausel, E. and Knopoff, L., Interpretation of Sa for a shield structure, Geophys. J. R. Astr. Soc., 36, p. 787, 1974.

Stauber, D. A., and D. M. Boore, Crustal thickness in northern Nevada from seismic refractive profiles, Bull. Soc. Am., 68, p. 1049, 1978.

Stephen, G. and B. L. Isacks, Toward an understanding of Sn: normal modes of low waves in an oceanic structure, Bull. Seism. Soc. Am., 67, p. 69, 1977.

TABLE 1. Great Basin Model

Layer Thickness H, km	Compressional Wave Velocity α, km/s	Shear Wave Velocity β, km/s	Density ρ, g/cm^3
2.5	3.55	2.05	2.20
22.5	6.10	3.57	2.82
10.0	6.60	3.85	2.84
29.0	7.80	4.50	3.30
40.0	7.80	4.12	3.30
16.0	7.81	4.10	3.40
20.0	7.85	4.05	3.40
20.0	7.87	4.05	3.42
20.0	7.92	4.06	3.44
20.0	8.00	4.38	3.46
20.0	8.10	4.41	3.48
20.0	8.20	4.44	3.49
60.0	8.35	4.53	3.53
60.0	8.66	4.70	3.58
60.0	8.96	4.90	3.63
60.0	9.29	5.13	3.75
60.0	9.65	5.34	3.91
60.0	9.97	5.53	4.05
100.0	10.31	5.76	4.21
100.0	10.71	6.03	4.40
100.0	11.10	6.23	4.56
	11.35	6.31	4.63

TABLE 2. Crustal Higher Modes

Event	Path	Period	Equivalent Crustal Thickness
1/30/68	Winn.-Dug	5 sec	26 km
5/29/68	Adel -Dug	6.8 sec	34 km
	Adel -TNP	6.7 sec	33.5 km
	Adel -Ren	5 sec	26 km
6/ 4/68	Adel -Dug	6.7 sec	33.5 km
	Adel -TNP	6.7 sec	33.5 km
	Adel -Ren	5.0 sec	26 km
6/ 5/68	Adel -Dug	6.7 sec	33.5 km
	Adel -Ren	5.0 sec	26 km
4/26/69	Boise-Ren	8.5-6.5 sec	37 km

FIGURE CAPTIONS

Figure 1. Location map showing events analysed and area studied; insert shows the relationship of the paths for which data was analyzed.

Figure 2. Seismograms recorded at Reno and Tonopah for an earthquake off Vancouver Island. The Sa phase is shown as a pulse preceding the fundamental mode Rayleigh wave arrival.

Figure 3. Seismograms for regional Great Basin earthquakes. For the Adel, Oregon earthquake seismogram recorded at Dugway, Utah, the higher mode data analyzed are the monochromatic wave train preceding the fundamental mode Rayleigh wave. For the central Idaho earthquake seismogram recorded at Reno, Nevada, the crustal higher mode analyzed is the earlier arriving dispersed wave train.

Figure 4. Theoretical seismograms for the Great Basin model calculated for epicentral distances appropriate to the observed data. Both the Sa phase and the crustal higher mode are present and in agreement with the observed period, phase velocity, and group velocity.

Figure 5. Rayleigh wave dispersion curves for the Great Basin model. The observed Sa phase corresponds to energy propagating primarily as the third higher Rayleigh mode.

Figure 6. Energy density diagram for the third higher Rayleigh mode at T=12.25 sec and C=4.54 k/s. The upper lob is confined primarily to the mantle lid.

Figure 7. Rayleigh wave group velocity curves for the GREAT BASIN model. The group velocities observed for the crustal higher mode data are indicated by short line segments.

Figure 8. Summary of dispersion results. Map indicates average crustal thickness along paths from higher, crustal mode data; inset shows lithospheric structure from Sa phase velocity data.

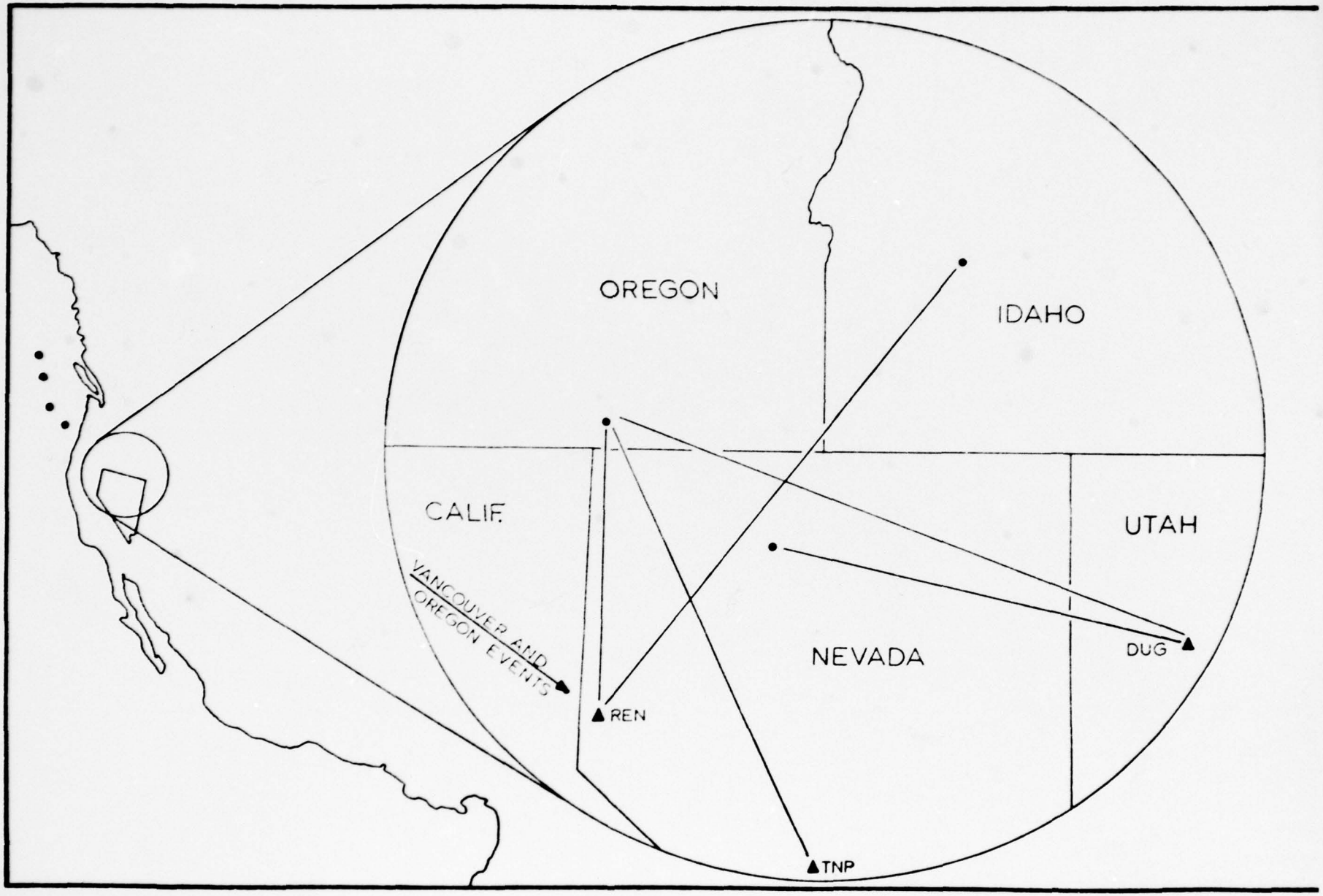
OREGON
IDAHO
CALIF.
UTAH
NEVADA
VANCOUVER AND OREGON EVENTS
REN
TNP
DUG

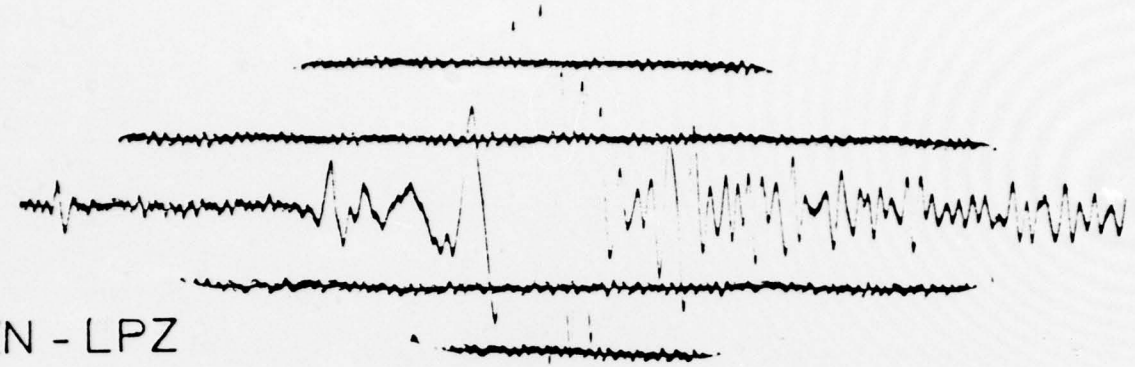

REN - LPZ

TNP - LPZ

VANCOUVER ISLAND REGION

FEB 1,1968 07 58 03.5 GMT 50.0° N 129.8° W

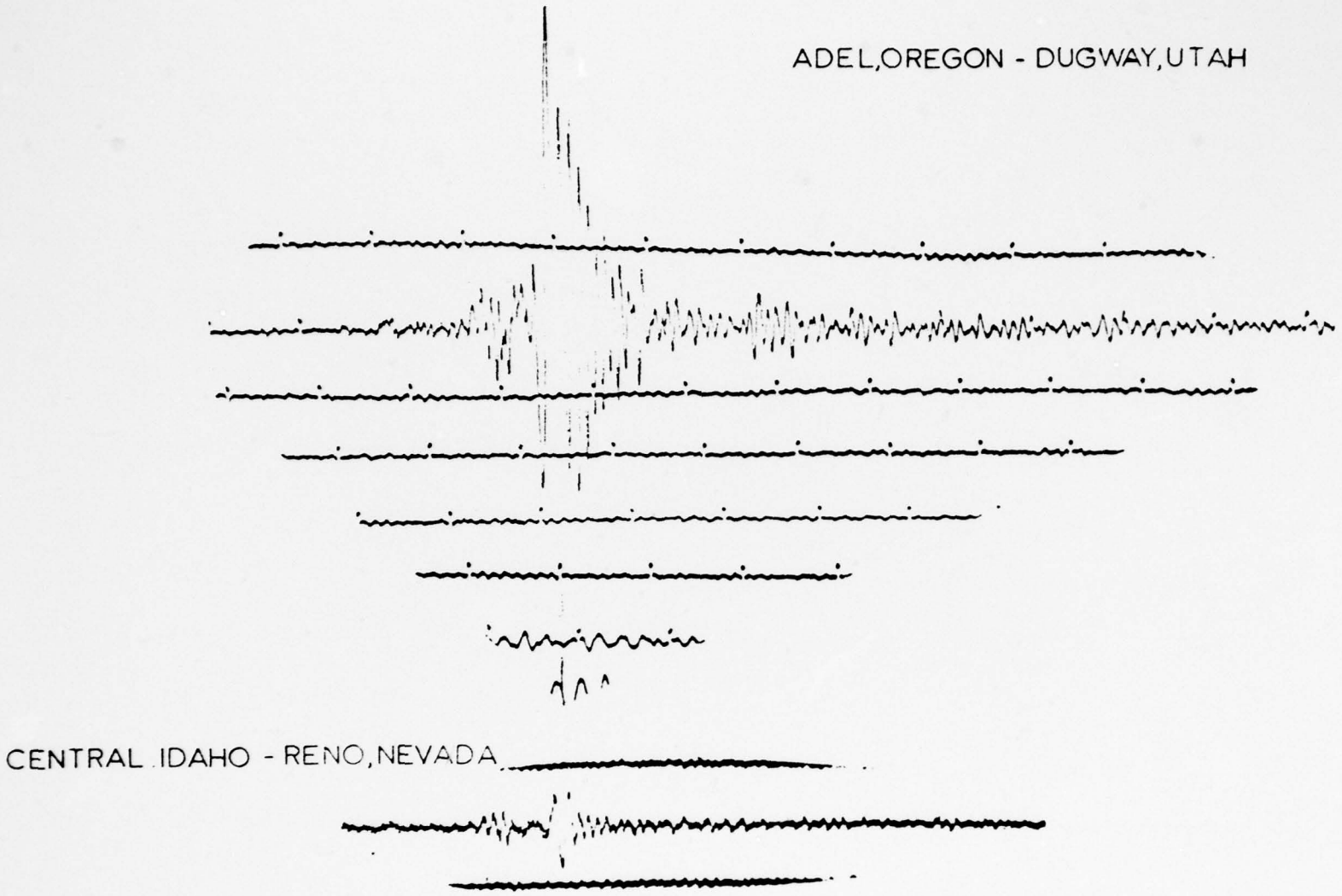
ADEL,OREGON - DUGWAY,UTAH
CENTRAL IDAHO - RENO,NEVADA

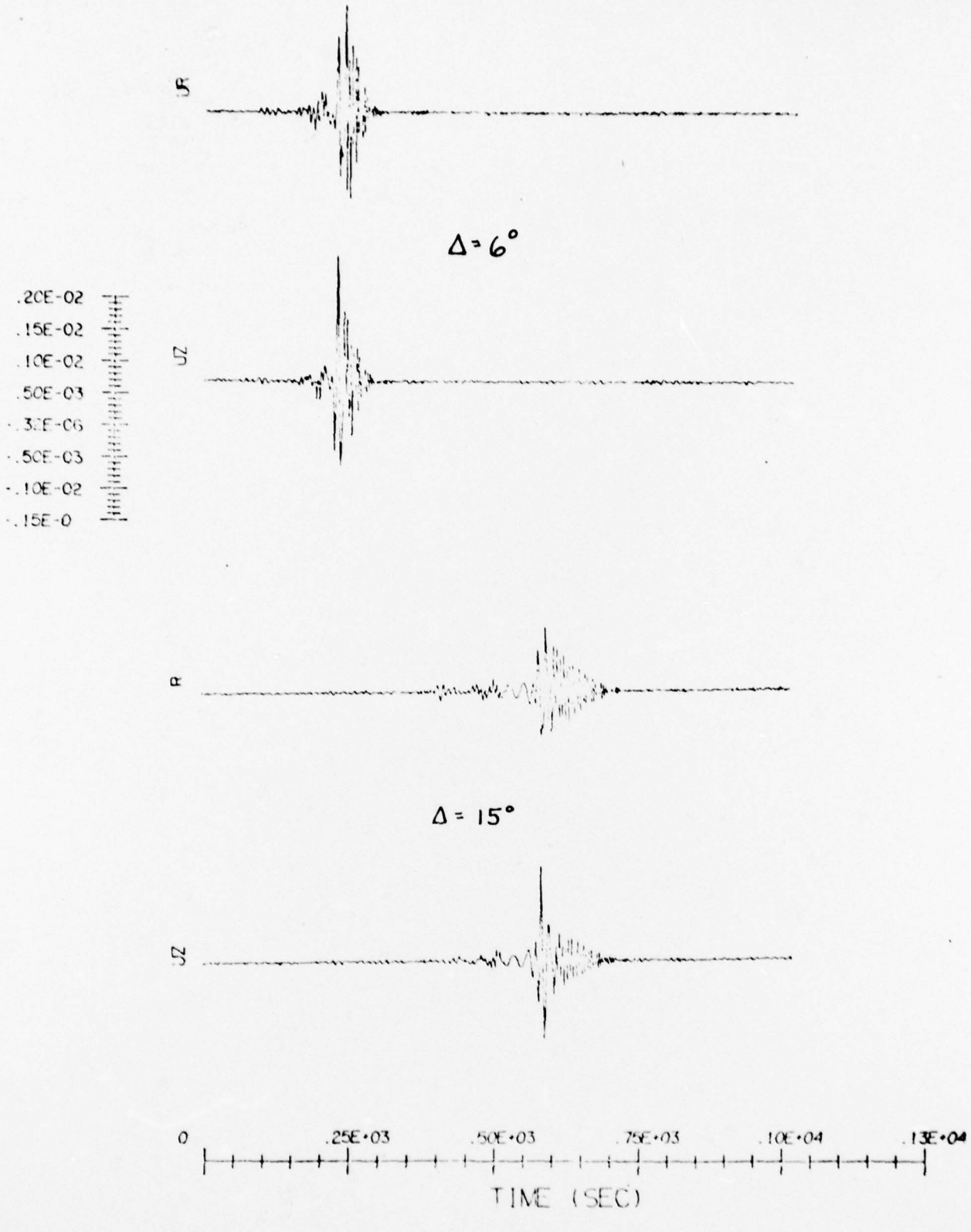
SR
Δ = 6°
.20E-02
.15E-02
.10E-02
.50E-03
.30E-06
-.50E-03
-.10E-02
-.15E-0
SZ
R
Δ = 15°
SZ
0
.25E+03
.50E+03
.75E+03
.10E+04
.13E+04
TIME (SEC)

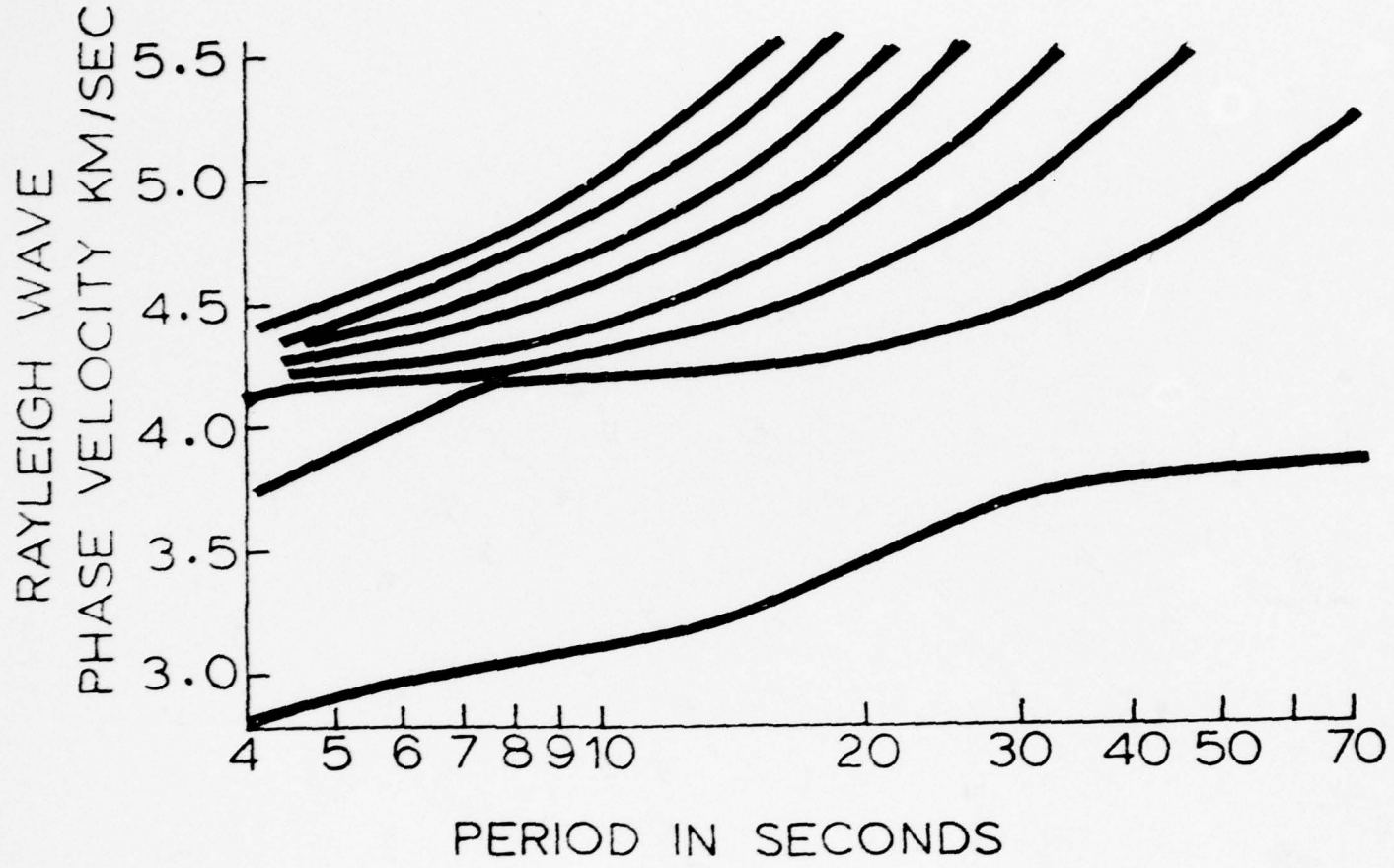
RAYLEIGH WAVE
PHASE VELOCITY KM/SEC
5.5
5.0
4.5
4.0
3.5
3.0
4 5 6 7 8 9 10 20 30 40 50 70
PERIOD IN SECONDS

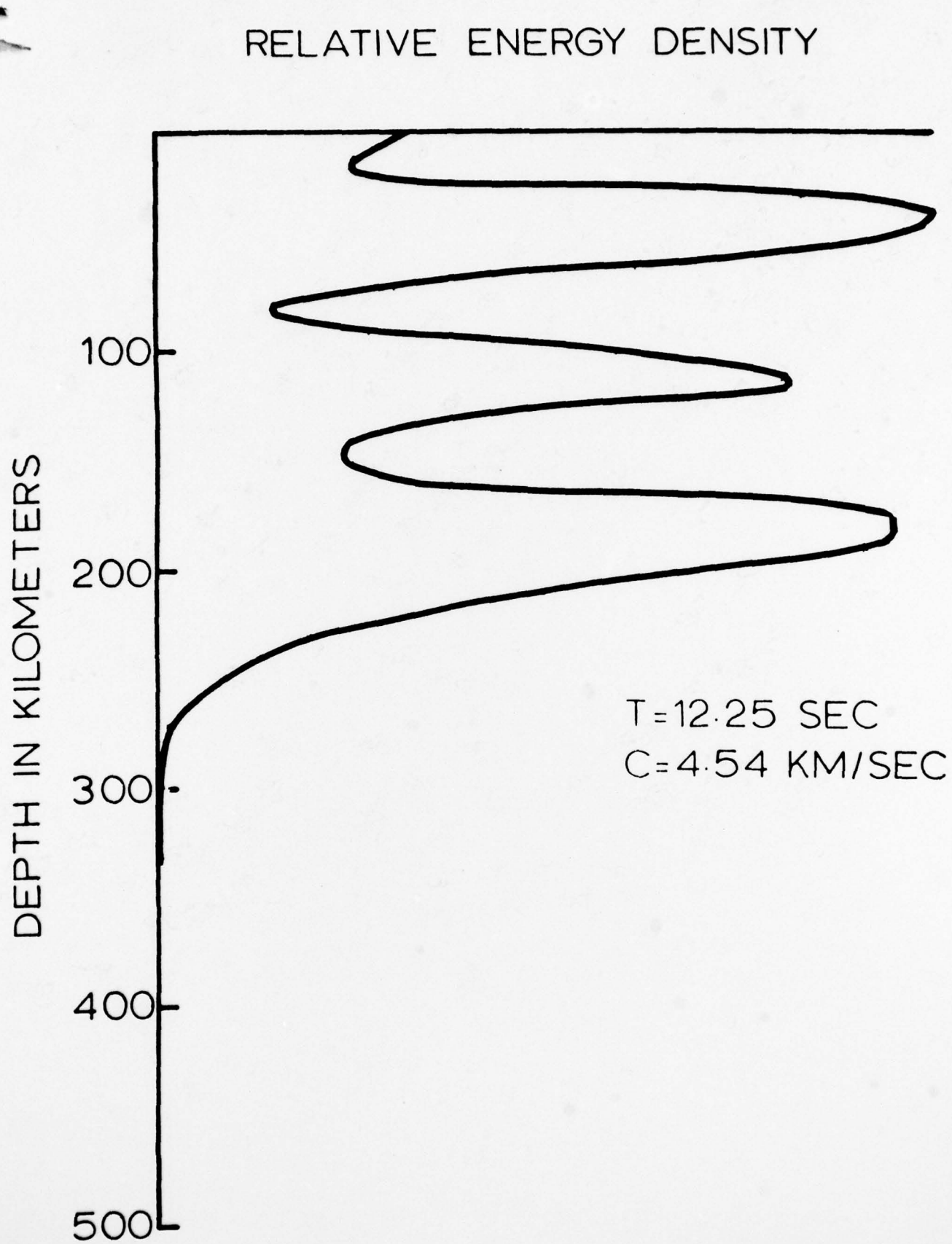
RELATIVE ENERGY DENSITY
DEPTH IN KILOMETERS
100
200
300
400
500
T=12.25 SEC
C=4.54 KM/SEC

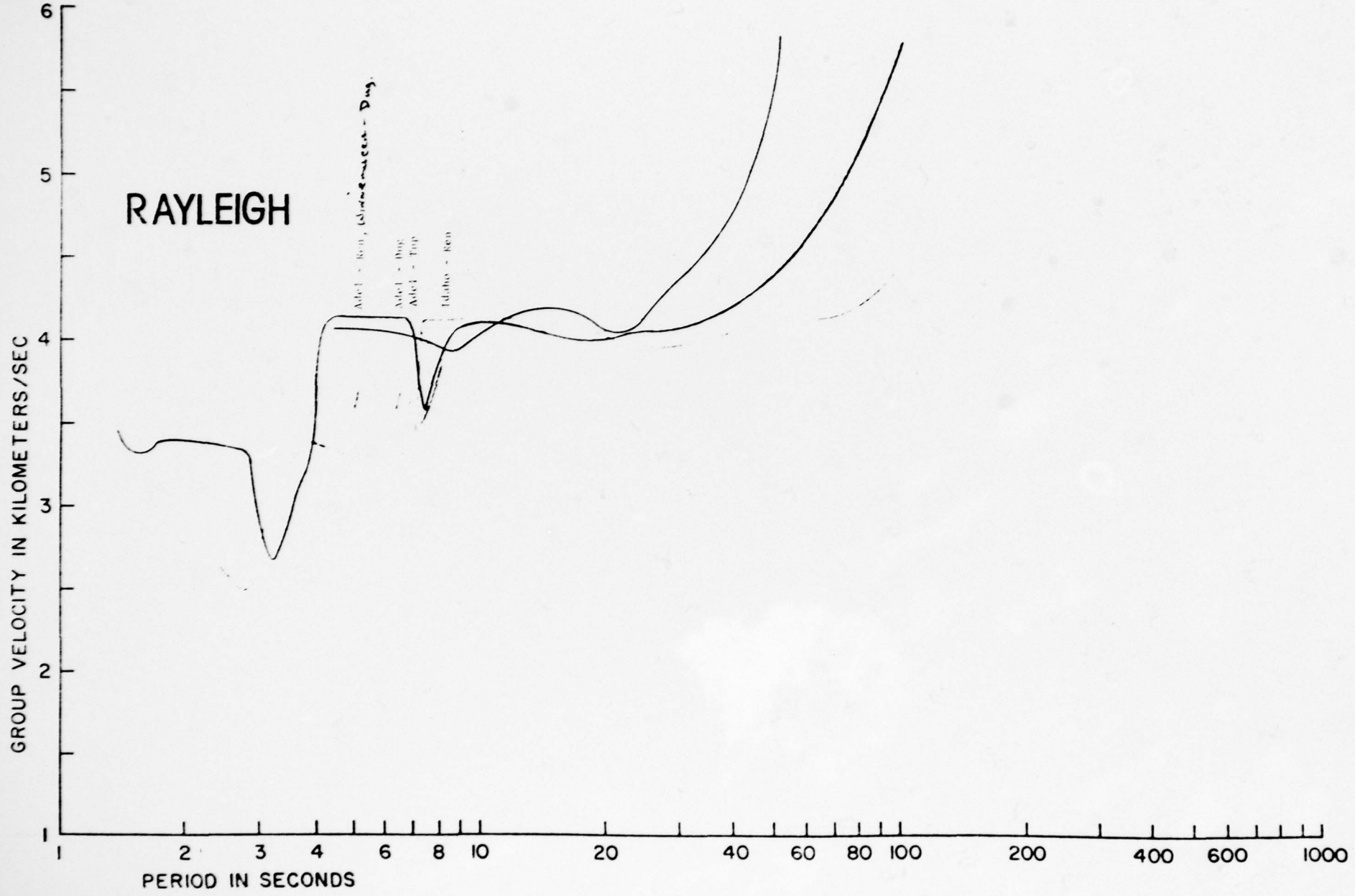
RAYLEIGH
GROUP VELOCITY IN KILOMETERS/SEC
PERIOD IN SECONDS
1
2
3
4
5
6
1
2
3
4
6
8
10
20
40
60
80
100
200
400
600
1000

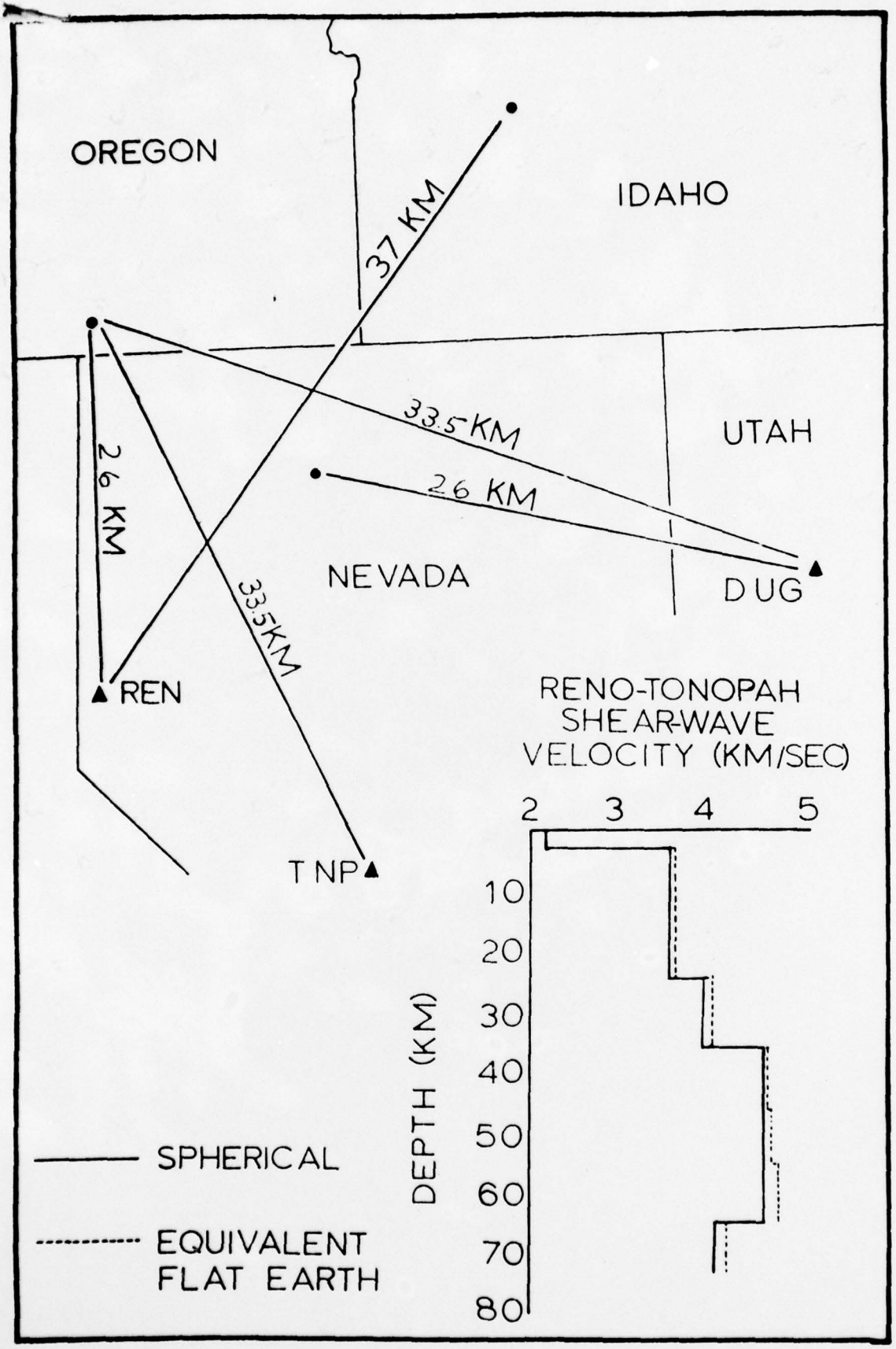
OREGON
IDAHO
UTAH
NEVADA
37 KM
33.5 KM
26 KM
26 KM
33.5 KM
REN
TNP
DUG
RENO-TONOPAH
SHEAR-WAVE
VELOCITY (KM/SEC)
2
3
4
5
10
20
30
40
50
60
70
80
DEPTH (KM)
SPHERICAL
EQUIVALENT
FLAT EARTH

SECURITY CLASSIFICATION OF THIS PAGE (When Data Entered)

REPORT DOCUMENTATION PAGE

READ INSTRUCTIONS BEFORE COMPLETING FORM

1. REPORT NUMBER: AFOSR-TR-79-0685	2. GOVT ACCESSION NO.
3. RECIPIENT'S CATALOG NUMBER	
4. TITLE (and Subtitle): SURFACE WAVES, SEISMIC REFRACTION AND UPPER MANTLE STRUCTURE OF THE BASIN AND RANGE	5. TYPE OF REPORT & PERIOD COVERED: Semiannual technical Interim rept. no. 3, 1 Feb 77-30 Sept 78
6. PERFORMING ORG. REPORT NUMBER	
7. AUTHOR(s): Keith F. Priestley	8. CONTRACT OR GRANT NUMBER(s): F49620-77-C-0070, ARPA Order-3291
9. PERFORMING ORGANIZATION NAME AND ADDRESS: Seismological Laboratory, Mackay School of Mines, University of Nevada, Reno, NV 89557	10. PROGRAM ELEMENT, PROJECT, TASK AREA & WORK UNIT NUMBERS: TF10-7F10, 61102E
11. CONTROLLING OFFICE NAME AND ADDRESS: Advanced Research Projects Agency /NMR, 1400 Wilson Blvd., Arlington, VA 22209	12. REPORT DATE: 3 April 1979
	13. NUMBER OF PAGES: 74
14. MONITORING AGENCY NAME & ADDRESS (if different from Controlling Office): Air Force Office of Scientific Research /NP, Bolling Air Force Base, Washington, D.C. 20332	15. SECURITY CLASS. (of this report): Unclass.
	15a. DECLASSIFICATION/DOWNGRADING SCHEDULE

16. DISTRIBUTION STATEMENT (of this Report)

Approved for public release; distribution unlimited.

17. DISTRIBUTION STATEMENT (of the abstract entered in Block 20, if different from Report)

18. SUPPLEMENTARY NOTES

19. KEY WORDS (Continue on reverse side if necessary and identify by block number)

Surface wave dispersion, refraction, Basin and Range, mantle structure

407 259

20. ABSTRACT (Continue on reverse side if necessary and identify by block number)

Body wave travel-times, surface wave dispersion, and gravity data have been used to refine the structural details of the crust and upper mantle within the northern Basin and Range. The crust varies in thickness from 35-40 km SE of Reno to 28 km in the western Battle Mountain heat flow high and 45-50 km in central Oregon. The mantle lid structure derived from fundamental mode surface wave data has been confirmed by higher mode surface wave data. Fundamental and higher mode dispersion data for southern Nevada and Arizona indicate the structure of the southern Basin and Range is similar to that of the Great Basin.

DD FORM 1 JAN 73 1473 EDITION OF 1 NOV 65 IS OBSOLETE

UNCLASSIFIED